Exogenous Stress and runs on perpetual futures: A global games approach.

Ravi Joshi*

January 21, 2026

Abstract

I illustrate the corrosive effects of marginal increase in adverse selection costs in the perpetual futures market and show how it can lead to run on open interest. Perpetual futures, 93% of crypto derivatives volume, rely on funding rates as their primary arbitrage mechanism to anchor prices to spot markets. Using the Terra, FTX, and SVB collapses as natural experiments, I document that similarly severe crises produce disproportionate impact on arbitrage functionality and run behavior. Applying global games, I model investors' stay-or-exit decisions as functions of public signals (spot volatility) and private signals (adverse selection costs), identifying a volatility threshold where adverse selection's effect on open interest flips from stabilizing to destabilizing, triggering a run. Only during Terra's collapse did Ethereum volatility exceed this threshold (1.8%/hour); open interest fell 65%, funding rates ceased correcting the basis, and arbitrage broke down. My main contribution is to highlight the importance of small departures from publicly observed signals, and what kinds of departures matter for runs in perpetual futures. My findings bridge limits-to-arbitrage with the global games run framework.

---

*rjosh15@lsu.edu

1 Introduction

Perpetual futures (perps), constituting approximately 93% of the crypto derivative's trading volume, with daily flows often exceeding $100 billion[1], are a type of derivative contract that enables traders to speculate on the price of an asset—like Bitcoin, Ethereum, or other cryptocurrencies—without needing to buy or own the underlying asset itself. The market's scale is substantial: Bitcoin and Ethereum together represent approximately 70% of total perpetual futures open interest, with combined positioning exceeding $125 billion in 2025 and annual trading volume surpassing $58 trillion in 2024. Yet leverage creates fragility: amplified exposure can precipitate runs through cascading liquidations. Understanding when and why such runs occur requires examining the unique structure of these instruments.

Unlike traditional futures contracts, perpetual futures don't have an expiration date, meaning traders can hold their positions indefinitely Shiller (1993), as long as they maintain the required margin. Because of no expiration date, there is no guaranteed date when the futures price would converge to the spot price. The fundamental mechanism anchoring perpetual futures to spot markets is the funding rate [2], a periodic cash flow between long and short positions that incentivizes arbitrageurs when the perpetual deviates from the underlying Angeris et al. (2023). When futures trade above spot, long positions periodically fund shorts, and vice versa, thereby closing the price deviations between perp and spot. In essence, the funding rate is the primary arbitrage mechanism in perpetuals.

In well-functioning markets, funding rates effectively enforce price parity He et al. (2022). However, during periods of market stress, this stability mechanism may fail. I exploit major collapse episodes in cryptocurrency markets as plausibly exogenous shocks to Ethereum perpetual futures as natural experiments to study the arbitrage mechanism in perpetual futures markets: the collapse of the Terra stablecoin ecosystem, the failure of the crypto exchange FTX, and the run on Silicon Valley Bank (SVB). These stress episodes are remarkably similar in duration and severity, each destroying comparable market value within a week [3]. Terra and FTX collapsed within three days, while the SVB episode unfolded over two days. Ethereum perpetuals on Kraken exchange provide a

---

[1]https://business.cornell.edu/article/2025/02/perpetual-futures-contracts-and-cryptocurrency/
[2]https://www.binance.com/en/support/faq/detail/360033525031
[3]($40B Terra, $32B FTX, $42B SVB)

clean laboratory to examine high-frequency funding–basis dynamics because funding is settled hourly, allowing us to measure funding adjustments at an hourly interval; by contrast, many major venues typically settle funding every eight hours.

First, I study the arbitrage mechanism of these new asset classes by examining funding rates during normal and stress periods. I show that the funding rate remains uniform during normal periods but becomes volatile and drops sharply once the crash begins. These patterns are consistent across all stress episodes examined. Post-crash, funding rates revert toward pre-crisis levels, indicating that arbitrage activity recovers sufficiently to restore basis discipline. Next, I examine funding-rate elasticity across market regimes. Funding-rate elasticity measures how closely the funding rate responds to the futures–spot basis and is estimated as the coefficient from regressing funding rates on the basis. A theoretical elasticity of one corresponds to full arbitrage pass-through, under which funding rates adjust proportionally to deviations between perpetual and spot prices. I therefore use funding-rate elasticity as an empirical measure of arbitrage effectiveness. Prior to the Terra collapse, the estimated elasticity is approximately 0.64, indicating partial but stable arbitrage activity. During the May 7–9 Terra crash, elasticity collapses to 0.38, consistent with a sharp deterioration in arbitrage effectiveness. Post-crash, elasticity rebounds to 0.91, suggesting a rapid restoration of arbitrage discipline once market stress subsides. In contrast, during the FTX and SVB stress episodes, funding-rate elasticity remains high and in several windows exceeds one. Pre FTX and SVB crashes, I see a stable and near-proportional relation between funding rate and the basis. During the crash period, the funding mechanism remained highly elastic but was subject to a level shift— funding rates increased (futures were trading above(SVB), below(FTX) spot), and the arbitrage mechanism was closing the basis. Post-crash, funding rates became negative (Terra and SVB), but funding elasticity stabilized, consistent with a restoration of equilibrium.

My central finding is an anomaly across otherwise comparable stress events: while funding rates decline sharply in all episodes, only a subset exhibits arbitrage collapse. While the Terra collapse is associated with a breakdown in funding-rate elasticity and hence a failure of the arbitrage mechanism, the FTX and SVB episodes preserve arbitrage effectiveness despite similarly severe market stress. This divergence highlights that not all market crashes impair the arbitrage mechanism in perpetual futures markets. A natural driver of this anomaly is plausibly the availability of capital required to close the basis. I examine open interest surrounding the crash episodes. Open

interest, the total number of outstanding contracts that remain unsettled, captures the aggregate leveraged exposure of market participants, including arbitrageurs. I find that the three crisis events exhibit starkly different open interest dynamics that align precisely with their differential arbitrage effectiveness patterns.

During the Terra collapse, Ethereum's open interest experienced a catastrophic collapse. From a stable pre-crash level averaging $58.7 million in notional value, open interest briefly spiked to $66 million before plummeting to just $21 million—a 65% decline that persisted throughout the post-crash period with minimal recovery. This provides evidence of a run on open interest and is suggestive of a fundamental breakdown in market-making and arbitrage infrastructure. In sharp contrast, the FTX bankruptcy and SVB failure displayed remarkable resilience in open interest despite their comparable or even greater systemic importance. During the FTX crisis, open interest increased only marginally from $9.5 million to over $13 million, and exceeded pre-crisis levels. The SVB episode showed even greater stability, with open interest fluctuating by just $0.75 million during the crash period. These differential patterns in market participation directly map to our funding-rate elasticity findings: arbitrage effectiveness collapse during Terra's episode coincides with the run on open interest, while maintained effectiveness during FTX and SVB reflects the persistence in open interest to intermediate basis divergences.

To examine differential run dynamics in open interest across stress episodes in Ethereum perpetual futures markets, I employ the global games framework of Goldstein and Pauzner (2005) and Morris and Shin (2001). Specifically, I examine the impact of marginal change in adverse selection costs on open interest, conditional on underlying market forces. Several studies have explored the role of adverse selection in market breakdown Kirabaeva (2010); Morris and Shin (2012); Chiu and Koeppl (2016). Adverse selection arises because some participants in financial markets have private information or superior expertise in evaluating new financial instruments and markets. In normal times, when the fraction of low-quality assets (i.e. the "lemon") is small, adverse selection does not have a significant effect on the market. However, during stress episodes, if the fraction of lemons is large or potential buyers believe it may be large, then even small increases in adverse selection can lead to a market breakdown. In this context, information costs manifest as adverse selection costs-the compensation market makers demand for expected losses when trading against better-informed counterparties Glosten and Milgrom (1985). Information asymmetry creates

strategic complementarities among market participants: when adverse selection costs are high, each investor rationally anticipates that others may possess superior information about fundamental value shifts, leading to a run on open interest Brunnermeier and Pedersen (2005)).

In my empirical estimation, adverse selection costs capture investors' beliefs about the fundamentals or asset quality. During normal periods, adverse selection costs are primarily driven by heterogeneous private information. During crisis episodes, however, adverse selection no longer operates as a purely private signal and instead becomes an equilibrium object jointly determined with public volatility. On the other hand, spot volatility σ_t and other market variables primarily act as a public signal. Open interest is the aggregate outcome of individual stay-or-exit decisions. The interaction between volatility and adverse selection costs in my model, therefore, provides an empirical analogue of the global-games run mechanism. A potential concern with the identification strategy is that adverse selection costs may be correlated with spot volatility, as both respond to underlying information flows Grundy and McNichols (1989); Van Ness et al. (2001). I view this correlation not as a threat to identification but as central to the run mechanism itself. In normal times, adverse selection reflects idiosyncratic private information. During systemic stress, adverse selection costs spike because market makers face elevated uncertainty about counterparty beliefs about asset quality and fundamental values, the same forces driving volatility. The interaction term in my specification captures precisely this crisis-specific amplification. My empirical contribution is documenting that this amplification crosses a threshold only during Terra's collapse, triggering a run, while remaining below threshold during FTX and SVB despite comparable market stress.

I find that a threshold level of spot volatility σ^* exists such that, when volatility is below σ^*, marginal increases in adverse selection costs are absorbed by open interest. Once volatility exceeds σ^*, the effect of the marginal increase in adverse selection costs turns negative: deterioration in beliefs about fundamentals or asset quality is associated with a sharp contraction in open interest, consistent with run equilibrium. I uncover a distinctive pattern only during the Terra crash, adverse selection costs become significant conditional on volatility, with volatility (σ^*) threshold of approximately $\approx 1.8\%$ per hour at which adverse selection costs do not impact open interest. Below this threshold, adverse selection costs are associated with higher open interest. But once volatility spikes past σ^*, the sign flips, and adverse selection costs put negative pressure on open interest, consistent with significant deleveraging that I find. In contrast, FTX and SVB episodes do not

exhibit a statistically or economically meaningful σ^* and open interest remains stable, suggesting that not all crashes push perpetual futures into the run region consistent with the global-games framework Goldstein and Pauzner (2005).

The robustness of this run mechanism is further validated through an out-of-sample test using the 2021 China regulatory crackdown, an event that introduced sudden, policy-driven information asymmetry. Consistent with the findings during Terra collapse episode, the crackdown's initial phase (Phase I) saw a sharp collapse in funding elasticity and a significant 45% decline in open interest, accompanied by the robust identification of a statistically significant threshold ($\sigma^* \approx 4.6\%/\text{hour}$) which was breached only during this phase of high information asymmetry. Crucially, the σ^* threshold was statistically insignificant during the subsequent phases of the China crackdown (Phases II, III, and IV), mirroring the results of the FTX and SVB periods where the run was not triggered and open interest remained stable. This replication across an independent, policy-driven shock confirms that the run on perpetuals is dependent on this endogenous run threshold, providing strong support for limits to arbitrage Shleifer and Vishny (1997).

In the final part of the paper, I examine the impact of the run on the funding mechanism. I show that when open interest collapses, the pass-through from basis to funding rate, the measure of arbitrage effectiveness, declines sharply. In other words, runs on open interest weaken the arbitrage functionality. This mechanism should be relevant for equity, FX, and commodity futures markets during stress episodes and connects the global-games run mechanism directly to the functioning of the core pricing anchor mechanism in derivatives.

The rest of the paper is organized as follows: Section 2 provides the literature review. Section 3 presents data and summary statistics. Section 4 presents empirical methodology. Section 5 presents results. Section 6 presents robustness tests. Section 7 concludes.

2   Literature Review

The arbitrage mechanism anchoring perpetual futures to spot markets is crucial for market efficiency, yet it is inherently vulnerable to the classic "limits to arbitrage" documented in financial theory. The earliest work by Grossman and Stiglitz (1980) established that fully efficient markets are impossible if information acquisition is costly, creating a fundamental limit on how closely prices

can track fundamentals. More formally, Shleifer and Vishny (1997) showed that capital constraints on arbitrageurs, such as funding constraints, can cause asset prices to deviate persistently from fundamental value. The idea of perpetual futures was formalized in academic literature by Shiller (1993), but the practical application of Shiller (1993) concept lay dormant until cryptocurrency exchanges operationalized perpetual futures, sparking a new wave of research in this direction. While recent research on perpetuals Ackerer et al. (2024); He et al. (2022); Gornall et al. (2024) establish the general effectiveness of the arbitrage mechanism, they leave open the question of how and why it fails during systemic crises, a gap this paper aims to fill.

The central mechanism investigated in this paper is the endogenous failure of arbitrage driven by runs using the global games approach. This framework, formalized by Morris and Shin (2001) and applied to banking by Goldstein and Pauzner (2005), models agents' decisions (to stay or run) as strategic complements, where individual action is dependent on the perceived actions of others. In these models, a unique run threshold (θ^*) exists, based on the interaction between a public signal and private signals. When the public signal crosses this threshold, strategic complementarities flip, leading to a run. My paper applies this framework to model the investors' 'stay-or-exit' decision in the perpetual futures market, by providing a reduced-form model to capture the run threshold. Morris and Shin (2012) demonstrates how small adverse-selection frictions can lead to the total breakdown of trade in an asset market; I empirically examine this mechanism in perpetual futures markets.

In conventional asset classes (FX, commodities, etc.), perpetual futures have not been traded in practice, but analogous principles exist. The closest parallel is the forward/futures pricing parity enforced by arbitrage. For example, in FX markets, Covered Interest Parity (CIP) ensures that the forward exchange rate is tied to the interest rate differential between currencies; any deviation is quickly arbitraged away under normal conditions. Du et al. (2018) document how CIP famously failed during the 2008 crisis, with forward prices diverging from parity by dozens of basis points as credit risk and funding constraints impeded arbitrage. I extend this literature by examining the same mechanism in the crypto derivative market. De Blasis and Webb (2022) compare the contract design and microstructure of Bitcoin quarterly futures versus perpetual futures. They document episodes where arbitrageurs could exploit mispricings between the two markets, but as crypto markets matured, those opportunities became less frequent. Kim and Park (2025) provide a

theoretical framework for setting the funding rate process optimally and discusses path-dependent funding and hedging for exchanges to ensure the perp price stays aligned with the underlying.

Streltsov and Ruan (2022) focus on how the introduction of perpetuals changes market behavior. Using natural experiments, they found that when exchanges added perpetual futures, trading activity surged and those markets attracted more informed traders. Alexander et al. (2020) examine BitMEX Bitcoin futures (both the perpetual swap and fixed-maturity quarterly futures) and find that the BitMEX perpetual plays a dominant role in price discovery for Bitcoin, often leading the spot market. Their results also suggest the periods of information inefficiency, where futures and spot diverge, profitable hedging and arbitrage opportunities are created. Broadly, several papers have explored the role of arbitrage in digital assets Liu et al. (2023); Joshi (2025); Makarov and Schoar (2020); Lyons and Viswanath-Natraj (2023). I extend the literature by examining the arbitrage mechanism in perpetual futures during periods of systemic stress. Most importantly, I extend literature on classical limits to arbitrage Shleifer and Vishny (1997); Grossman and Stiglitz (1980) by showing that capital constraints can be triggered endogenously, and I provide an empirical application of global games run thresholds Goldstein and Pauzner (2005); Morris and Shin (2001) to the perpetual futures market.

3   Data & Sample Construction

I utilize minute-by-minute trade and perpetual futures data for the Ethereum/USDC pair from Kaiko, a leading provider of cryptocurrency data Makarov and Schoar (2020). The data spans 2020 through 2023, encompassing multiple stress episodes. I use data for the Kraken exchange because its hourly funding AsiaNext Exchange (2024) provides me with a setup to examine high-frequency data. I compute market microstructure variables from ETH–USDC trade data and aggregate them hourly. Following Hasbrouck (1993), the realized volatility of Ethereum prices, $\sigma_{ETH,t}$, is obtained using a 24-hour rolling window of hourly close-to-close price changes. This estimator adjusts for the bias induced by bid-ask bounce and provides an estimate of the efficient price volatility. This approach builds on the model of Roll (1984) but directly estimates the volatility of the efficient price rather

than the spread. The variable is measured in USD and is computed as:

$$\sigma_{ETH,t} = \sqrt{\text{Var}(\Delta P_t) + 2, \text{Cov}(\Delta P_t, \Delta P_{t-1})}, \qquad \Delta P_t = \ln\left(\frac{\text{Close}_t}{\text{Close}_{t-1}}\right). \qquad (1)$$

I compute hourly returns, $Returns_t$, as the logarithmic price change from the previous hour, capturing short-term return persistence.

$$Returns_t = \ln\left(\frac{\text{Close}_t}{\text{Close}_{t-1}}\right), \qquad (2)$$

Order flow imbalance, $OF_{i,t}$, measures net buying pressure as the signed volume imbalance within each hour,

$$OF_{i,t} = \frac{\sum_{j \in t} q_j V_j}{\sum_{j \in t} |V_j|}, \qquad (3)$$

where $q_j \in \{+1, -1\}$ indicates buyer- or seller-initiated trades and V_j is the trade volume.

3.1 Estimation of Adverse Selection

The measure of information asymmetry follows Glosten and Harris (1988) framework to compute adverse selection, which estimates the adverse-selection component of the bid–ask spread by regressing price changes on trade direction and trade size. Accordingly, I denote the unobserved true price of the asset by m_t. It represents the price of the asset assuming a fully competitive market maker and no inventory costs or clearing fees. Innovations in m_t, therefore, result from public news or information arrival through order flows. More formally,

$$m_t - m_{t-1} = e_t + Q_t Z_t, \qquad (4)$$

with $Q_t = 1(-1)$ for a buyer- (seller-) initiated trade. In Equation 4, e_t represents the impact of public news, and Z_t is the market maker's compensation for bearing the adverse selection risk. Hence, Z_t is the adverse selection component of the bid-ask spread. The observed prices reflect factors such as the market maker's monopoly power, inventory costs, and clearing fees. To account

8

for these factors, Glosten and Harris (1988) include a second component in their specification, called the *transitory component*. Formally,

$$P_t = m_t + Q_t C_t, \tag{5}$$

where the dependence of the transitory component on the trade direction reflects the fact that market makers buy low and sell high.

Larger trades increase the bid-ask spread through both components. Therefore, I allow Z_t and C_t to depend on the volume, V_t. Glosten and Harris (1988) assume a linear dependence to facilitate the estimation.

$$Z_t = z_0 + z_1 V_t$$
$$C_t = c_0 + c_1 V_t$$

Substituting these into Equation 5 and taking the first difference gives

$$P_t - P_{t-1} = c_0(Q_t - Q_{t-1}) + c_1(Q_t V_t - Q_{t-1} V_{t-1}) + z_0 Q_t + z_1 Q_t V_t + e_t. \tag{6}$$

I estimate the parameters in Equation 6 for every trading hour. I observe all the variables in Equation 6 in the data and can estimate the parameters, c_0, c_1, z_0, and z_1 through OLS regressions.[4] Using the estimated parameters, $\hat{c}_0, \hat{c}_1, \hat{z}_0$, and $\hat{z}_1$, I calculate $\hat{C}_t$ and $\hat{Z}_t$ for each trade. My measure of the adverse selection component of the bid-ask spread for the trading hour h is

$$Adverse\ Selection_h = \sum_{t \in h} \hat{Z}_t$$

---

[4]Contrary to Glosten and Harris (1988), I can observe the trade direction (Q_t) in my data. Furthermore, the rounding error in prices is negligible in my setup, given the minuscule tick size on Exchanges (0.00000010 for BTC/USD pair). Therefore, I do not resort to the maximum likelihood method to estimate the parameters.

All variables are computed hourly and lagged one period when used as predictors in the model. Next, I compute hourly adverse selection costs, such as:

$$\text{AS Cost}_t = \text{RawAS}_{[t-1 \to t]} \times \left(\frac{\text{Volume}_t^{24h}}{\text{Price}_t} \right),$$

where $\text{RawAS}_{[t-1 \to t]}$ denotes the median adverse-selection component between $t-1$ and t (in USD/ETH), Volume_t^{24h} is the 24-hour notional trading volume (in USD), and Price_t is the spot ETH price (USD/ETH).

3.2 Summary Statistics

Table 1 reports summary statistics for Ethereum spot and perpetual markets across three major disruption events: the Terra/Luna collapse (May 2022), the FTX bankruptcy (November 2022), and the Silicon Valley Bank (SVB) failure (March 2023). Each event is partitioned into pre-crisis, crisis, and post-crisis windows, allowing for a cross-event comparison of market microstructure dynamics under extreme stress. All statistics are based on hourly observations. Adverse selection costs are reported in scaled units of cost per \$10,000 notional per hour; specifically, the table entries must be multiplied by 10^4 to obtain the underlying cost. For example, an entry of 1.69 corresponds to an underlying adverse-selection cost of $1.69 \times 10^4 = 16,900$ USD per hour.

Funding-rate and basis dynamics reveal distinct patterns in market positioning across events. In Terra, the mean funding rate rises from approximately 0.002 in the pre-crisis window to about 0.01 during the crash, before turning negative in the post-crisis period (0.002). Combined with a shift in the average basis from mildly positive (0.17) to more elevated levels (0.32) during the crash, then slightly negative (0.05) afterward, this pattern is consistent with an initial buildup of leveraged long positions supporting arbitrage, followed by broad deleveraging once the peg breakdown becomes persistent.

By contrast, the FTX episode is characterized by persistently negative funding rates and deeply negative bases. The mean funding rate falls from −0.003 pre-crisis to around −0.02 in the crash window and remains negative post-crisis. The basis moves from a modest discount (−0.11) to a much larger one (−0.85) during the crash, before settling at an intermediate discount (−0.47) post-crisis.

10

This pattern reflects sustained short pressure and a prolonged period in which perpetual prices trade at a discount to the index. The SVB disruption shows a more modest but highly asymmetric dislocation: the pre-crisis basis is slightly positive (0.16), turns mildly negative in the crash window (-0.06), and collapses to a large discount (-2.65) in the post-crisis period, indicating persistent pricing stress even after the immediate failure window.

Volatility and transaction costs rise across all three events. Measured by σ_{ETH}, average volatility roughly doubles in the crash window for both Terra and FTX (from about 1% to 2%), and increases from roughly 0.5% to 1% for SVB. Post-crisis, volatility normalizes quickly for FTX, falling back toward pre-crisis levels, but remains at or above pre-crisis levels for Terra and especially SVB.

Bid-ask spreads and adverse selection-driven trading costs (market makers' risk premia) show particularly strong stress patterns once the scaling is taken into account. For Terra, the mean risk premia rises from 2700 USD in the pre-crisis window to 18,400 USD during the crash, before falling to 3600 post-crisis. FTX displays the same qualitative pattern: Risk premia rises from 6,800 to 14,000 USD during the crash and then drops to 1,800 post-crisis. SVB exhibits a smaller but still meaningful increase in adverse selection costs from 700 pre-crisis to 1,800 USD in the crash window, followed by a modestly higher post-crisis level of 2,200. Across all events, market makers' risk premia becomes markedly more expensive.

Open interest and order flow highlight differences in market participation and the depth of available capital across events. Terra exhibits a dramatic collapse in mean open interest, from 58.74 million pre-crisis to 49.27 million during the crash and just 20.30 million post-crisis, implying a sharp contraction in the capital to absorb price and funding-rate shocks. In contrast, FTX shows a mild increase in open interest from 10.96 to 11.33 million in the crash window and to 11.83 million post-crisis, suggesting that some capital remained engaged or was even attracted by the dislocation. SVB features a gradual erosion of open interest (from 9.36 to 9.05 and then 8.94 million), consistent with a more conventional risk-off retrenchment.

Order-flow imbalances become more negative during all three crisis windows, reflecting the dominance of aggressive selling pressure. Terra's mean order flow moves from approximately zero (0.002) pre-crisis to a clearly negative value (0.07) during the crash, before turning positive (0.08) post-crisis, suggesting net buying interest as prices stabilize at lower levels. FTX shifts from slightly positive order flow (0.06) before the collapse to negative order flow (0.04) in the crash window,

and remains marginally negative thereafter, consistent with continued net selling and unwinding of long exposure after the bankruptcy. SVB displays the most severe deterioration in order flow in relative terms, declining from 0.10 pre-crisis to 0.25 in the crash period, with only a partial recovery (0.04) post-crisis. These patterns underscore that microstructure responses are highly event-specific, shaped by the nature of the underlying shock and the resilience of available capital.

4 Empirical Setting

4.1 Arbitrage Mechanism

I examine how closely the perpetual funding rate tracks the basis around the stress episodes. My analysis centers on the fundamental arbitrage relationship that governs perpetual contract pricing, where funding payments serve as the primary mechanism for anchoring derivative prices to their underlying spot values. To understand the arbitrage mechanism, I examine the funding rates during stress regimes. The funding rate consists of two components: a fixed interest rate and a dynamic component (premium) that adjusts to the basis. The variation in the dynamic component captures the efficacy of arbitrage mechanism. Funding-rate elasticity captures how closely the dynamic component of the funding rate adjusts to the basis, and is computed as the coefficient from regressing funding rates on the basis. Since the interest rate is fixed, the coefficient of regression captures the impact of variations in dynamic rates on the basis. A theoretical elasticity of one implies that the arbitrage mechanism fully aligns the perpetual price with the spot price and effectively closes the perp-spot gap.

$$f_t = f^{\text{fix}} + f_t^{\text{dyn}}. \tag{7}$$

$$\frac{\partial f_t}{\partial t} = \frac{\partial f_t^{\text{dyn}}}{\partial t}, \tag{8}$$

Following He et al. (2022) to quantify the degree of futures–spot mispricing and assuming $r - r' \approx 0$ (a reasonable approximation since there is no interest on ETH holdings), the annualised

no-arbitrage deviation measure in ETH, ρ, for each minute can be computed as

$$\rho_t \approx \kappa \left(\log F_t - \log S_t\right).$$

where F_t denotes the perpetual futures price and S_t represents the spot index value at time t. The scaling factor emerges from the institutional structure of cryptocurrency perpetual markets in Kraken, where funding payments typically occur at hourly intervals (24 times times daily). The annualization thus requires:

$$\kappa = \underbrace{24}_{} \text{ payments/day} \times \underbrace{365}_{} \text{ days/year} = 8760 \text{ hours/year} \tag{9}$$

This scaling transforms minute-level basis observations into annualized percentage rates, facilitating economic interpretation. I utilize minute-by-minute Ethereum/USD perpetual futures data from Kraken, spanning 2020 through 2023, encompassing multiple stress episodes. Kraken's hourly funding AsiaNext Exchange (2024) provides an ideal laboratory for examining funding-basis dynamics at high frequency. The dataset includes the perpetual futures price F_t, the corresponding spot index price S_t, the funding rate f_t applied to positions, as well as trading activity metrics like open interest, bid–ask spreads, and volume. Following exchange conventions, the hourly funding rate f_t is settled at the end of each hour, while the contemporaneous basis is defined as the log difference between mark and index prices. The mark price is the exchange's internal fair-value estimate of the perpetual contract. The index price represents the reference spot value of ETH/USD.

$$b_t = \ln(\text{mark}_t) - \ln(\text{index}_t). \tag{10}$$

I construct an evenly spaced one-hour panel and compute the average premium over the preceding hour,

$$\bar{b}_{t-1:t} = \frac{1}{60} \sum_{s \in [t-1,t)} b_s, \tag{11}$$

which serves as the explanatory variable for the next-hour funding payment. Both funding and basis are expressed in annualized units by multiplying by $\kappa = 24 \times 365 = 8760$. The baseline regression

is

$$f_t^{APR} = \alpha + \beta \rho_t^{APR} + \varepsilon_t, \tag{12}$$

where $\rho_t^{APR} = \kappa \bar{b}_{t-1:t}$ represents the annualized premium, and β captures the elasticity of the dynamic component of the funding rate, $\beta = \frac{\partial f_t^{\text{dyn}}}{\partial \rho_t^{APR}}$.

The coefficient β captures the funding-basis elasticity—the percentage change in funding rates associated with a one percentage point change in the annualized basis. In a frictionless benchmark with fully effective arbitrage, we would expect $\beta = 1$, meaning funding adjusts one-for-one with the basis and fully transmits price discrepancies into funding incentives. Values of β below 1 indicate under reaction: funding does not adjust enough to close the basis, suggesting a weakened or constrained arbitrage channel. Values of β above 1 indicate overreaction: funding moves more than one-for-one relative to the basis, consistent with an aggressive response in which the funding mechanism strongly rewards (or penalizes) positions and draws in additional arbitrage activity.

4.2 Run Mechanism

The empirical model is motivated by global-games run frameworks in the spirit of Morris and Shin (2001); Goldstein and Pauzner (2005). In those models, agents decide whether to *stay* or *run* based on their heterogeneous private beliefs (information) about the fundamental state θ_t and the homogeneous public information. Investors' decisions are driven by the interaction between public and private information structures that give rise to a unique threshold θ^* at which the decision switches from no-run to run. I map this structure to the perpetual market as follows:

- The *fundamental* is the investor perception about asset quality. The higher the belief that "lemons" exist, the lower the fundamentals. Each investor faces *private information costs* captured as the adverse selection cost per trade. This measure captures market makers' risk premia from trading against better-informed counterparties. The higher the adverse selection costs, the lower the fundamentals. It plays the role of a *private signal* to market participants.

- I proxy market resilience by short-horizon spot volatility σ_t. Higher σ_t indicates a more fragile trading environment with greater execution and margin risk. Volatility σ_t is uniformly observed by all market participants and therefore acts as a *public signal*.

- Open interest OI_t is the aggregate outcome of individual stay-or-exit decisions. A run on open interest corresponds to a sharp decline in OI_t as many arbitrageurs simultaneously choose to exit.

Investors choose whether to maintain or liquidate their position based on this information structure. Under standard assumptions, the equilibrium can be characterized by a threshold rule: for a given level of public stress σ_t, investors exit when their adverse selection costs exceed a cutoff. The capital outflow, open interest decline, is a function of public and private signals.

4.2.1 Reduced-Form Specification for Open Interest

Rather than estimating a structural global game, I work with an empirical reduced-form representation of the equilibrium relationship between open interest, market frictions, and adverse selection costs. I estimate coefficients as

$$OI_t = \alpha + \beta_{AS} \cdot \text{AS\_cost}_{t-1} + \beta_\sigma \cdot \sigma_{t-1} + \beta_{AS \times \sigma} \cdot \text{AS\_cost}_{t-1} \times \sigma_{t-1} + \gamma' X_{t-1} + \mu_{h(t)} + \varepsilon_t, \ (13)$$

where:

- OI_t is open interest (in millions of USD) in the ETH perpetual at hour t;

- AS_cost_t is the adverse selection cost ;

- σ_t is the spot volatility of ETH;

- $\text{AS\_cost}_t \cdot \sigma_t$ is the interaction that captures state-dependence of the effect of heterogeneous information costs on open interest;

- X_t are controls (such as order-flow imbalance, and returns);

- $\mu_{h(t)}$ are hour-of-day fixed effects;

- ε_t is an error term.

Equation (13) can be interpreted as a local linear approximation to the global-games equilibrium mapping from the public signal σ_t and the distribution of private information costs (summarized by AS_cost$_t$) into the aggregate outcome OI_t. The key nonlinearity implied by global games theory is that the impact of information costs on the equilibrium mass of "stayers" (investors that keep positions) is *state-dependent*: beyond a certain level of public stress, small changes in private information can trigger a run.

4.2.2 Adverse Selection Costs and Volatility Threshold

I focus on the impact of marginal change in information costs on the investors' action, conditional on the public signal. In my specification, the marginal effect of adverse selection costs on open interest is given by the partial derivative of OI_t with respect to AS_cost$_t$:

$$\frac{\partial OI_t}{\partial \text{AS\_cost}_t} = \beta_{AS} + \beta_{AS \times \sigma} \cdot \sigma_t. \tag{14}$$

Equation (14) has a simple interpretation:

- For a fixed level of volatility σ_t, $\frac{\partial OI_t}{\partial \text{AS\_cost}_t}$ measures the expected change in available capital (open interest) associated with a marginal increase in information costs.

- If $\frac{\partial OI_t}{\partial \text{AS\_cost}_t} > 0$, the market can absorb higher information costs without losing available capital; adverse selection is not yet "run-inducing."

- If $\frac{\partial OI_t}{\partial \text{AS\_cost}_t} < 0$, higher information costs are associated with a decline in open interest; adverse selection becomes *capital-destructive* and is consistent with a run on positions.

A central implication of global-games models is the existence of an equilibrium threshold (the public signal) at which investor behavior changes and a regime shift happens (run equilibrium). In my reduced-form representation, this threshold is captured by the volatility level at which the marginal effect of adverse selection on open interest switches sign. Equating (14) to zero yields the *threshold volatility*. The volatility threshold σ^* in (15) is then the empirical analogue of the global-games run threshold: a level of public stress at which a marginal increase in private information costs changes from stabilizing to destabilizing for open interest.

$$\frac{\partial OI_t}{\partial \text{AS\_cost}_t} = 0 \quad \implies \sigma^* = -\frac{\beta_{AS}}{\beta_{AS \times \sigma}} \tag{15}$$

For σ^* to be a strong and valid threshold, β_{AS} and $\beta_{AS \times \sigma}$ must be of opposite signs and be statistically significant - the implied σ^* in (15) is positive. This delivers the global-games–style threshold:

$$\frac{\partial OI_t}{\partial \text{AS\_cost}_t} = \begin{cases} > 0, & \text{if } \sigma_t < \sigma^* \to No\ Run \\ < 0, & \text{if } \sigma_t > \sigma^* \to Run \end{cases} \tag{16}$$

When $\sigma_t < \sigma^*$, marginal increases in adverse selection costs are absorbed by available capital; the market remains in a "no-run" region. Once σ_t exceeds σ^*, the sign flips, and increases in adverse selection costs are associated with declines in open interest, consistent with withdrawal of the capital. In my empirical work, I estimate (13) separately for distinct stress episodes (Terra, FTX, SVB, and the 2021 China ban phases) and compute σ^*. I then compare the location of σ^* relative to realized volatility and the behavior of open interest across episodes.

5 Results

5.1 Baseline estimates

I begin by examining the evolution of the dynamic component of funding basis elasticity (β) for Ethereum perpetual contracts on Kraken from **September 2020 to April 2022**. This interval includes multiple market cycles, volatility regimes, and systemic stress events. I examine the funding–basis relation during normal market conditions to establish a baseline against which stress-period distortions can be measured. Establishing this benchmark is essential: it provides clear evidence of what "efficient" arbitrage looks like during calm market periods.Figure 1b displays the scaled elasticity series across this 20-month window. The subsequent stress events—Terra's collapse, the FTX bankruptcy, and the SVB collapse can therefore be interpreted as deviations from this baseline. Table 2 presents baseline results for arbitrage functionality. I find that, in the calm periods, the mapping between the prior-hour premium and next-hour funding rate is stable and

consistent, with funding payments from long to short most of the periods. This behavior is fully consistent with the functioning arbitrage mechanism during calm periods.

5.2 Funding Rate Dynamics during Market Stress

Do all market stress limit *"arbitrage"* in perpetual futures? I examine funding rates, a crucial *perp spot* price-convergence mechanism, during periods of extreme market stress. Figure 2 presents the 48-hour rolling average funding rate (annualized) across three distinct periods: the Pre-Crash, Crash, and Post-Crash periods, shaded in green, red, and blue, respectively. This is a period of stress transmission from the Terra, FTX, and SVB ecosystems to ETH derivatives markets. Funding rate remained stable pre-crash but shows a steep decline once the stress starts.

Next, I examine how closely the perpetual funding rate tracked basis around stress episodes. Understanding when and why funding elasticity breaks down can reveal deeper insights into the behavior of traders and the health of derivatives markets. Figure 3 shows the hourly relation between the next-hour funding rate and the prior-hour premium.

The baseline regression is.

$$f_t^{APR} = \alpha + \beta \rho_t^{APR} + \varepsilon_t, \tag{17}$$

where $\rho_t^{APR} = \kappa \bar{b}_{t-1:t}$ represents the annualized premium.

Figure (3, and 4) and Table 3 present results. Results suggest that the pre-Terra period exhibits $\beta = 1.44 \times 10^{-5}$ ($R^2 = 0.113$), corresponding to a scaled elasticity of 0.64. During the Terra crash (May 7–10), β is insignificant and declines to 0.64×10^{-5} ($R^2 = 0.11$), with a scaled elasticity of 0.38. An increase in the intercept [1.44 (pre) to 8.41(post)] indicates an increased response of the dynamic component of the funding rate. This suggests that arbitrageurs were attempting to close the basis; however, a decrease in elasticity (β) indicates that the arbitrage mechanism was ineffective in restoring the basis. In the post-crash phase (May 11–30), β increases to 1.52×10^{-5} ($R^2 = 0.13$), and the scaled elasticity rises to 0.91, consistent with restoration of arbitrage mechanism.

The pre-FTX period exhibits $\beta = 2.43 \times 10^{-5}$ ($R^2 = 0.64$), corresponding to a scaled elasticity of 1.44, indicating a strong and stable link between funding rates and the basis. The intercept is negative ($\alpha = -6.95 \times 10^{-6}$), implying that, on average, perpetual prices trade below spot and shorts pay longs even after controlling for the basis. During the FTX crash window (November 6–11),

18

β increases to 2.91×10^{-5} ($R^2 = 0.75$), with a scaled elasticity of 1.72, reflecting a temporary amplification of the pass-through from basis deviations to funding adjustments. At the same time, the intercept becomes more negative ($\alpha = -1.39 \times 10^{-5}$), indicating that the level of funding shifts further downward and that short positions pay a larger amount to longs during the crash. In the post-crash phase (November 12–December 15), β rises further to 3.18×10^{-5} ($R^2 = 0.91$), and the scaled elasticity reaches 1.88, consistent with a strengthened funding - basis linkage as markets stabilized, while the intercept remains negative ($\alpha = -9.97 \times 10^{-6}$), signaling a persistently discounted perp relative to spot and continued net payments from shorts to longs.

Silicon Valley Bank faced a rapid deposit run on March 8- 9, 2023, and was closed by regulators on March 10, 2023. Withdrawal requests of around \$42B (25% of deposits) hit within eight hours; end-of-day cash balance about –\$958M. Funding α turned more negative as balance sheets tightened and shorts demanded premia, but β did not break, so the arbitrage mapping still functioned like FTX. Around this failure, ETH perpetuals on Kraken exhibit a *tight funding - basis relation with a downward level shift*: the crash window scatter shows more negative funding for a given premium, while the elasticity remains near or above its pre-period level and only eases afterward. This mirrors the FTX episode in which arbitrage effectiveness is preserved. By contrast, during Terra's collapse, arbitrage effectiveness collapses.

5.3   Runs and Global Games Approach

Why would similarly devastating market events have opposite effects on funding rate elasticity? To understand the source of this anomaly, I analyze open-interest dynamics and interpret sharp and persistent contractions in open interest as runs on perpetual futures markets that impair the correction of basis deviations. Figure 5 plots the open interest rate every hour during the stress episodes. I find that open interest behaves very differently across crash episodes. During the Terra collapse, average ETH perpetual open interest falls from about \$58.7 million in the pre period to \$20.3 million in the post period—a decline of roughly 65%—with the crash window itself exhibiting both elevated volatility and extremely wide dispersion in open interest. By contrast, during the FTX bankruptcy and the SVB failure, ETH perpetual average open interest remains in a relatively narrow range: it drifts slightly *upward* from \$10.9m to \$11.8m across the FTX episode and declines by

only about 1% (from \$9.38m to \$9.28m) across the SVB window. In other words, only during the Terra crash period, there was a run on the ETH-perpetual market as seen by capital constraints to arbitrage.

To understand the cause of the run only during the Terra crash episode, I bring to this setting a global-games perspective in the spirit of Morris and Shin (2001); Goldstein and Pauzner (2005). In global games models, agents decide whether to stay or run based on a fundamental state and noisy private signals about that state, and a threshold emerges at which the unique equilibrium switches from no-run to run. I adapt this framework (Equation 16) by modeling investors' stay-or-exit decisions (change in open interest) as a function of public stress (volatility) and private signals (adverse selection and costs, see Table 4, and 5). Table 6 presents results for the global games reduced form model. During the Terra crash, I estimate $\beta_{AS} = 4.591$ (p<0.01) and $\beta_{AS \times \sigma} = -257.249$ (p<0.01), yielding a volatility threshold $\sigma^* = 1.785\%$ per hour (see Table 7). This threshold lies within the range of realized hourly volatility during the crisis, Terra crash median $\sigma = 0.71\%$, with peaks exceeding 1.8% for 37 hours (Fig 7). As σ_t crossed σ^*, the marginal effect of adverse selection on open interest flipped from positive to negative, triggering a withdrawal of open interest, a run equilibrium. Open interest collapsed by 65% (Figure 5a), consistent with a run regime. During the pre and post-crash periods, volatility remained below the threshold all the time, and open interest remained stable.

In stark contrast, during the FTX and SVB crash episodes, the run mechanism was not activated (Table 7 and Figures 8, 9). For FTX, $\beta_{AS \times \sigma}$ is statistically insignificant (-6.062, p>0.10), implying no meaningful threshold. For SVB, the interaction term is positive during the crisis (85.659, p>0.10), but the opposite sign is required for a run threshold. Consequently, even though volatility crossed the threshold in both events (FTX crash $\sigma = 0.9\%$, SVB crash $\sigma = 1.1\%$), adverse selection costs did not induce the same run dynamics. Moreover, during the SVB Collapse period, the threshold volatility of 1.1% was statistically significant post-crash, and volatility remained below this threshold before. Open interest remained stable (FTX: +36%; SVB: -4%) (Figure 5b, 5c), and the funding–basis elasticity stayed near or above 1, indicating preserved arbitrage functionality.

5.4 Runs on Open Interest and Arbitrage Breakdown

The preceding analysis establishes three facts: (i) open interest collapses during the Terra episode but remains stable or increases during FTX and SVB episodes; (ii) funding-rate elasticity breaks down during Terra but persists during FTX and SVB; (iii) only Terra episode exhibits a statistically significant run threshold σ^* that realized volatility breaches. I now directly test the mechanism linking these findings, whether runs on open interest impair the funding rate to correct basis deviations.

The funding rate mechanism requires arbitrage capital to function. Arbitrageurs holding positions absorb basis deviations and collect funding payments, ensuring that funding rates adjust to close the futures spot gap. When arbitrageurs exit en masse, the capital necessary to enforce price parity disappears. If runs are the mechanism through which arbitrage breaks down, open interest collapse should result in the breakdown of the arbitrage mechanism.

I estimate:

$$f_t = \alpha + \beta \cdot OI_{t-1} + \varepsilon_t \tag{18}$$

where f_t is the hourly funding rate (scaled to 10^6) and OI_{t-1} is lagged open interest (in millions USD). Under normal conditions, funding rates respond to the basis, and open interest should have limited explanatory power for funding rate levels. During a run, however, open interest becomes the binding constraint; as capital flees, the funding mechanism loses its corrective capacity. The coefficient β sign across episodes is central to understanding the impact of the runs on arbitrage effectiveness. Table 8 summarizes the patterns.

When $\beta > 0$ and significant during a crash, open interest and funding rates move together - both declining as arbitrageurs exit. When $\beta < 0$ and significant, open interest and funding rates move inversely - open interest increases while funding rates fall into negative territory. Arbitrageurs enter to exploit the dislocation, and the funding mechanism operates to attract this capital, consistent with arbitrage functioning. The sign and significance of β across crisis windows therefore provides evidence on whether run on open interest contributed to the arbitrage mechanism failure.

Table 9 presents the results. During the pre-crash period, open interest has no significant relationship with funding rates. The funding mechanism operates independently of the open interest, which is not a binding constraint. This changes sharply during the crash. Open interest becomes a

significant predictor of funding rates. The positive coefficient indicates that a run on open interest predicts funding rates collapse: as arbitrageurs exit, the funding rate's capacity to correct the basis deteriorates in tandem. This is direct evidence that the run on open interest impaired the arbitrage mechanism. Post-crash, with open interest stabilized at approximately $20 million, 65% below pre-crash levels, the relationship again becomes insignificant. The market reached a new equilibrium, but one with diminished capital.

The FTX episode presents a striking contrast. Open interest is highly significant across all periods, but the coefficient is negative and turns positive in the post-crash period. This reflects the market dynamics during the FTX period: Ethereum perpetual prices traded below spot, and funding rates turned negative, in which short positions paid long positions. As arbitrageurs entered the Ethereum perpetual market to exploit the funding opportunity, open interest increased. The negative β therefore indicates arbitrage functioning, not failing. Open interest rose from $9.5 million to over $13 million during the crash window (Figure 5b), a 36% increase. The funding mechanism continued to close the basis and arbitrage functionality were preserved.

The SVB episode reveals a more nuanced pattern. Open interest predicts funding rates across all windows with positive coefficients. The relationship intensifies during the crash; however, the underlying dynamics differ fundamentally from Terra. Open interest declined only modestly during the SVB crash (approximately 4%), then recovered within the same window (Figure 5c). The positive coefficient indicates that open interest and funding rates were jointly stressed, but the run did not materialize. This pattern aligns precisely with the threshold estimates in Table 7: during SVB, the run threshold σ^* was insignificant, and realized volatility did not trigger the global-games run equilibrium. SVB represents a stressed market in which there was a small contraction in open interest, but run was not triggered.

These findings establish that runs on open interest are the mechanism through which arbitrage breaks down in perpetual futures markets. The funding rate requires capital to function. When investors exit, capital flees, and the anchor fails. When investors enter or simply remain engaged, the mechanism persists even under extreme market stress.

6 Robustness

The phased China 2021 regulatory crackdown is a powerful natural experiment to test the limits of arbitrage under the global games framework. The ban is correctly seen, as recent work shows, as one of the sharpest regulatory shocks in crypto's history, causing a market-wide collapse in prices, a spike in volatility, and—most relevant for this study—plummeting market quality through mass liquidity withdrawal and forced exit of arbitrageurs. Manwaring (2021).

China's regulators progressively escalated restrictions on crypto activity from May to September 2021. On May 18, financial associations ordered banks and payment firms to halt all crypto-related services, citing financial-stability risks. On May 21, the State Council explicitly targeted Bitcoin mining and trading, triggering nationwide enforcement and shutdown orders across major mining provinces through June. By September 24, the PBoC and nine national agencies declared all crypto transactions illegal and barred foreign exchanges from serving Chinese users. The phased nature of regulatory announcements created an information-revelation sequence: initial policy ambiguity (Phase I) was gradually resolved through enforcement actions (Phases II–III) and culminating in a comprehensive, symmetric ban (Phase IV) as shown in Table 10.

I first show that the funding rate elasticity collapses towards zero (Fig 10 and Table 11), in Phase I, with the highest level of information asymmetry. During the pre-crackdown period, the funding mechanism operated with near-ideal efficiency ($\beta_{\text{scaled}} = 1.48$), where 30% of funding-rate variation was explained by observable basis deviations, consistent with well-functioning arbitrage markets. In Phase I, both funding elasticity collapses to 0; $\beta_{\text{scaled}} = 0.09$, $R^2 \approx 0$). The estimates indicate that the dynamic component of the funding rate (f_t^{dyn}) stops responding to mispricing. Elasticity recovers towards a value of one post Phase I period.

To understand the collapse in funding elasticity around the China crackdown, I examine open interest. A sudden decline in open interest implies a run on perpetual. (Figure 11). Prior to the ban, average open interest was about $72.7 million, with values ranging from $45.7 million to more than $102 million. During Phase I of the ban, open interest falls to $39.4 million—a decline of roughly 45% relative to the pre-ban mean—and the lower tail reaches levels near $20 million. In Phases II and III, open interest stabilizes at an even lower plateau of $27–31 million, before partially recovering in Phase IV (mean $77.3 million). Thus, the China ban episode features a discrete,

policy–driven run on ETH perpetual positions in Phase I, followed by a no-run regime in which open interest remained stable and increased during later phases.

I adapt the global games approach (Equation 16) to understand the cause of the collapse of open interest during Phase I and model investors' stay-or-exit decisions (change in open interest) as a function of public stress (volatility) and private signals (adverse selection costs). Results are presented in Table 13 and Figure 12. During Phase I, I estimate β_{AS} = 1.987 (p<0.01) and $\beta_{AS \times \sigma}$ = −42.837 (p<0.01), yielding a volatility threshold σ^* = 4.6% per hour. This threshold is statistically significant and lies within the range of realized hourly volatility during Phase I (Fig. 12, Terra crash median σ = 0.71%, with peaks exceeding 1.8% for 37 hours). As σ_t crossed σ^*, the marginal effect of adverse selection on open interest flipped from positive to negative, triggering a run. Open interest collapsed by 45% (Figure 11) soon after volatility crossed the threshold σ^* during Phase I. During other Phases, σ^* was statistically insignificant, and the run was not triggered despite volatility σ crossing the threshold σ^* during Phases III and IV. Results from Phase I (Table 11 and Figure 10) suggest that the funding rate could not correct the basis, and arbitrage broke down. Overall, these robustness checks confirm that the results are fully consistent with the patterns observed during the Terra, FTX, and SVB episodes, and they extend the global-games framework of Goldstein and Pauzner (2005); Morris and Shin (2001) and the limits-to-arbitrage insights of Shleifer and Vishny (1997) to an empirical setting in perpetual futures markets.

7 Conclusion

This paper applies the global games framework to identify when and why arbitrage mechanisms fail in derivatives markets. Our contribution to the literature is threefold. First, I document a new empirical puzzle: similar crises of comparable severity produce starkly opposite effects on arbitrage functionality. This finding suggests that the crisis magnitude alone may not fully determine run behavior, pointing to additional mechanisms at work. Second, I provide a theoretical resolution grounded in the global games run threshold equilibrium model. By mapping the global games framework onto perpetual futures markets, with spot volatility as a public signal, adverse selection costs as an an equilibrium object which originates from private information but whose variation becomes endogenously linked to public volatility during stress episodes, and open interest as the

aggregate outcome, I derive an endogenous volatility threshold that separates run regimes from non-run regimes by estimating the run equilibrium threshold. This threshold is empirically estimable and statistically significant only during Terra's collapse episode, precisely when arbitrage failed.

Third, I bridge two foundational literatures. I extend classical limits to arbitrage by showing that constraints can emerge endogenously, complementing capital shortage as an explanatory channel. Simultaneously, I provide an empirical application of global games run thresholds to the derivatives (perpetual futures) market by identifying the specific mechanism through which arbitrage breaks down under stress. My findings carry implications for exchange design, regulatory surveillance, and risk management: monitoring volatility relative to estimated thresholds may provide early warning of arbitrage mechanism failure before capital flight becomes visible.

References

Ackerer, D., Hugonnier, J., and Jermann, U. (2024). Perpetual futures pricing. Technical report, National Bureau of Economic Research.

Alexander, C., Choi, J., Park, H., and Sohn, S. (2020). Bitmex bitcoin derivatives: Price discovery, informational efficiency, and hedging effectiveness. *Journal of Futures Markets*, 40(1):23–43.

Angeris, G., Chitra, T., Evans, A., and Lorig, M. (2023). A primer on perpetuals. *SIAM Journal on Financial Mathematics*, 14(1):SC17–SC30.

AsiaNext Exchange (2024). Asianext crypto futures methodology overview. [https://www.asianext.c om/wp-content/uploads/2025/01/AsiaNext-Crypto-Futures-Methodology-Overview-Dec-202 4.pdf](https://www.asianext.com/wp-content/uploads/2025/01/AsiaNext-Crypto-Futures-Methodology-Overview-Dec-2024.pdf). Accessed: YYYY-MM-DD.

Brunnermeier, M. K. and Pedersen, L. H. (2005). Predatory trading. *The Journal of Finance*, 60(4):1825–1863.

Chiu, J. and Koeppl, T. V. (2016). Trading dynamics with adverse selection and search: Market freeze, intervention and recovery. *The Review of Economic Studies*, 83(3):969–1000.

De Blasis, R. and Webb, A. (2022). Arbitrage, contract design, and market structure in bitcoin futures markets. *Journal of Futures Markets*, 42(3):492–524.

Du, W., Tepper, A., and Verdelhan, A. (2018). Deviations from covered interest rate parity. *The Journal of Finance*, 73(3):915–957.

Glosten, L. R. and Harris, L. E. (1988). Estimating the components of the bid/ask spread. *Journal of financial Economics*, 21(1):123–142.

Glosten, L. R. and Milgrom, P. R. (1985). Bid, ask and transaction prices in a specialist market with heterogeneously informed traders. *Journal of financial economics*, 14(1):71–100.

Goldstein, I. and Pauzner, A. (2005). Demand–deposit contracts and the probability of bank runs. *the Journal of Finance*, 60(3):1293–1327.

Gornall, W., Rinaldi, M., and Xiao, Y. (2024). Funding payments crisis-proofed bitcoin's perpetual futures. *Available at SSRN*.

Grossman, S. J. and Stiglitz, J. E. (1980). On the impossibility of informationally efficient markets. *The American economic review*, 70(3):393–408.

Grundy, B. D. and McNichols, M. (1989). Trade and the revelation of information through prices and direct disclosure. *The Review of Financial Studies*, 2(4):495–526.

Hasbrouck, J. (1993). Assessing the quality of a security market: A new approach to transaction-cost measurement. *The Review of Financial Studies*, 6(1):191–212.

He, S., Manela, A., Ross, O., and von Wachter, V. (2022). Fundamentals of perpetual futures. *arXiv preprint arXiv:2212.06888*.

Joshi, R. (2025). Essays on stablecoins'stability.

Kim, J. and Park, H. (2025). Designing funding rates for perpetual futures in cryptocurrency markets. *arXiv preprint arXiv:2506.08573*.

Kirabaeva, K. (2010). Adverse selection, liquidity, and market breakdown. Technical report, Bank of Canada Working Paper.

Liu, J., Makarov, I., and Schoar, A. (2023). Anatomy of a run: The terra luna crash. Technical report, National Bureau of Economic Research.

Lyons, R. K. and Viswanath-Natraj, G. (2023). What keeps stablecoins stable? *Journal of International Money and Finance*, 131:102777.

Makarov, I. and Schoar, A. (2020). Trading and arbitrage in cryptocurrency markets. *Journal of Financial Economics*, 135(2):293–319.

Manwaring, K. (2021). The volatility implications of the chinese cryptocurrency ban. Graduate student research report, Utah State University. Accessed: Month Day, 2025.

Morris, S. and Shin, H. S. (2001). Global games: Theory and applications.

Morris, S. and Shin, H. S. (2012). Contagious adverse selection. *American Economic Journal: Macroeconomics*, 4(1):1–21.

Roll, R. (1984). A simple implicit measure of the effective bid-ask spread in an efficient market. *The Journal of finance*, 39(4):1127–1139.

Shiller, R. J. (1993). Measuring asset values for cash settlement in derivative markets: hedonic repeated measures indices and perpetual futures. *The Journal of Finance*, 48(3):911–931.

Shleifer, A. and Vishny, R. W. (1997). The limits of arbitrage. *The Journal of finance*, 52(1):35–55.

Streltsov, A. and Ruan, Q. (2022). Perpetual price discovery and crypto market quality. In *Perpetual Price Discovery and Crypto Market Quality: Streltsov, Artem| uRuan, Qihong*. [Sl]: SSRN.

Van Ness, B. F., Van Ness, R. A., and Warr, R. S. (2001). How well do adverse selection components measure adverse selection? *Financial Management*, pages 77–98.

Figure 1: Historical Funding–Basis Elasticity (Scaled β), ETH perpetual. The dashed line represents the theoretical benchmark $\beta = 1$. I plot the scaled funding–basis elasticity ($\beta_{\text{scaled}} = \beta/\text{median}(f_t/\rho_t)$) and funding rate over 20 months. The scaling adjustment is for better interpretation of dynamic funding elasticity. I see the value of funding elasticity consistently over the theoretical benchmark value during the period of key market events. The funding rate was consistently elevated from November 2020 to April 2021. A positive funding rate implies that the futures is over spot. An increase in the funding rate implies increased investors' participation. The $\beta \approx 1$ levels are consistent with an efficient pricing regime.
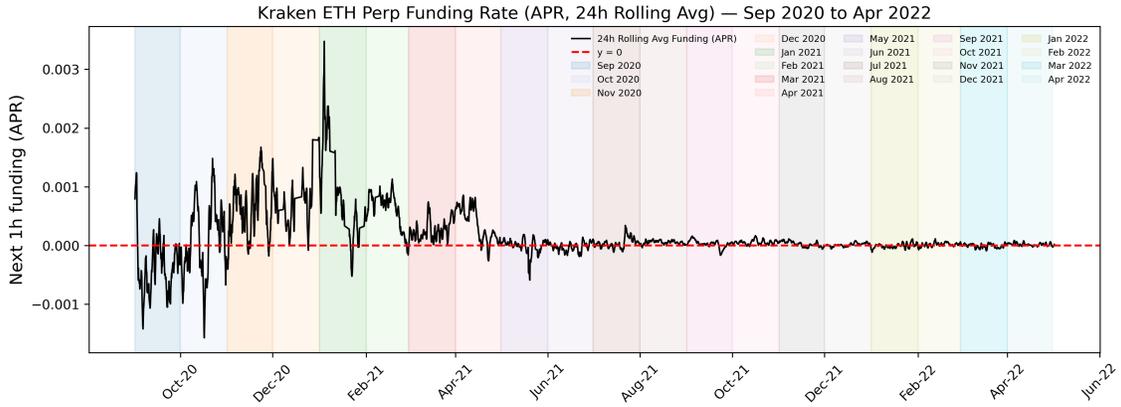

(a) 24-Hour Rolling Funding Rate
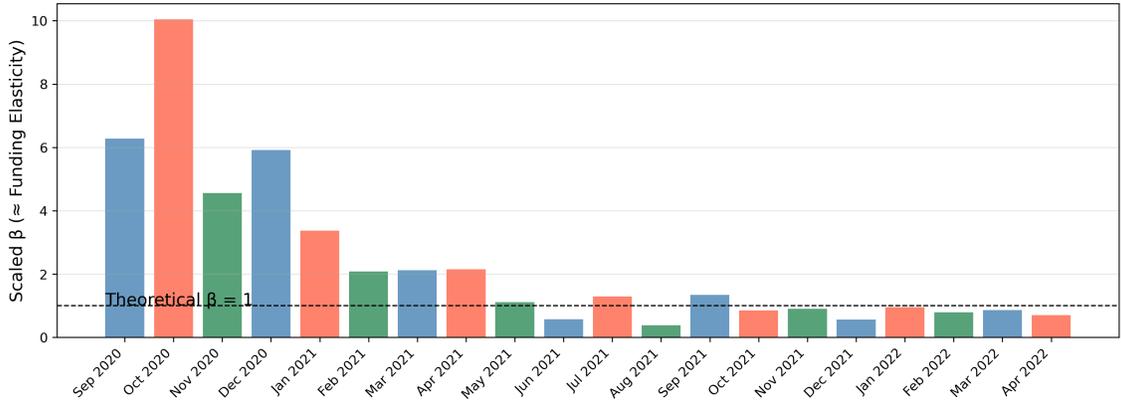
(b) Scaled Funding Elasticity

Figure 2: Kraken ETH Perpetual Funding Rates Around Major Market Crashes. Hourly annualized funding rates (APR) are shown for three crisis episodes: (a) Terra collapse (May 2022), (b) FTX collapse (Nov 2022), and (c) SVB collapse (Mar 2023). Shaded regions denote the event windows. Each episode shows a sharp deviation of funding from equilibrium levels, consistent with transient dislocations in the arbitrage mechanism. The red dotted horizontal line is the inflection point where the funding regime changes from Long to Short. Above the red line, futures trade over spot.
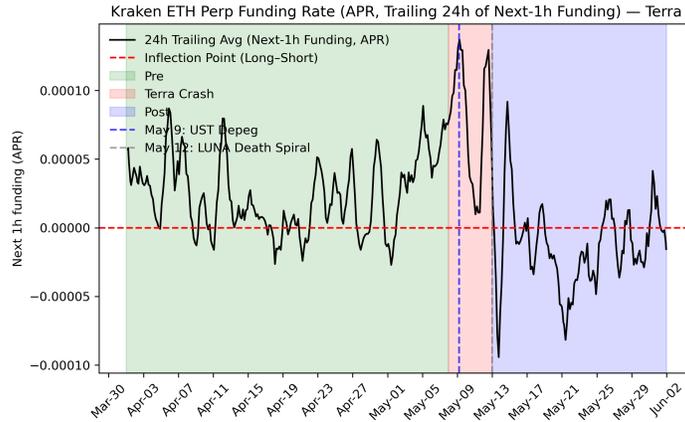
(a) Terra Crash Onset (May 9, 2022)
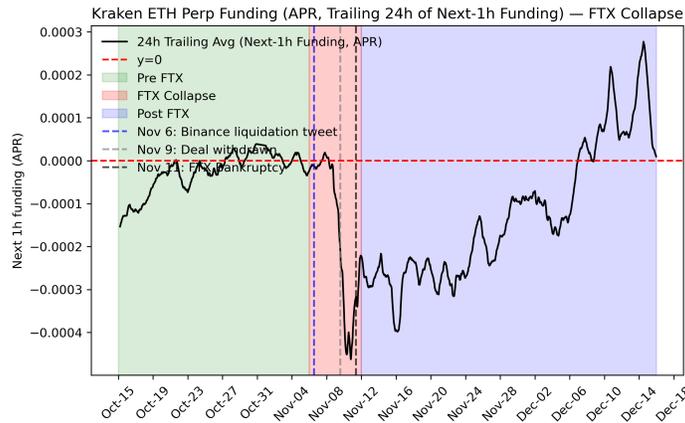
(b) FTX Collapse Onset (Nov 6, 2022)
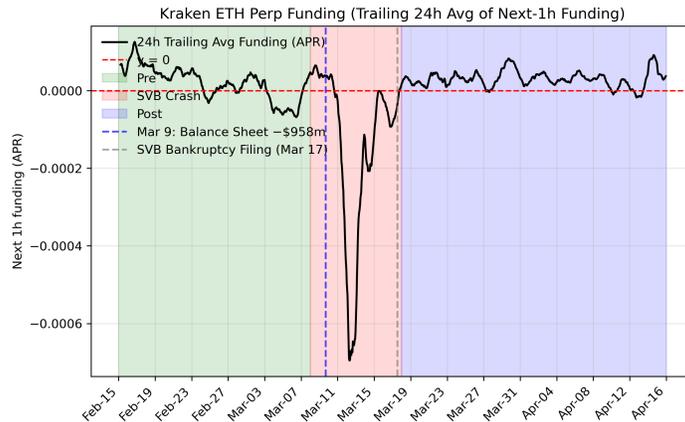
(c) SVB Collapse Onset (Mar 9, 2023)

Figure 3: Funding–premium elasticity on Kraken ETH perpetuals around major stress events.
Each panel plots next-hour funding (APR) vs. the prior-hour perp–spot premium (APR) for pre-, crash-, and post-event windows with within-window OLS fits: (a) Terra—flatter slope and higher dispersion (impaired arbitrage); (b) FTX—tight, nearly linear mapping with negative premium (shorts pay long); (c) SVB—downward level shift with slope largely preserved (funding-liquidity shock).
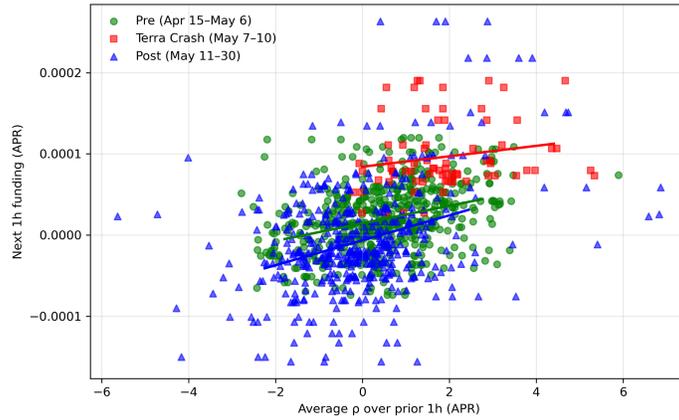
(a) Terra (May 9, 2022)
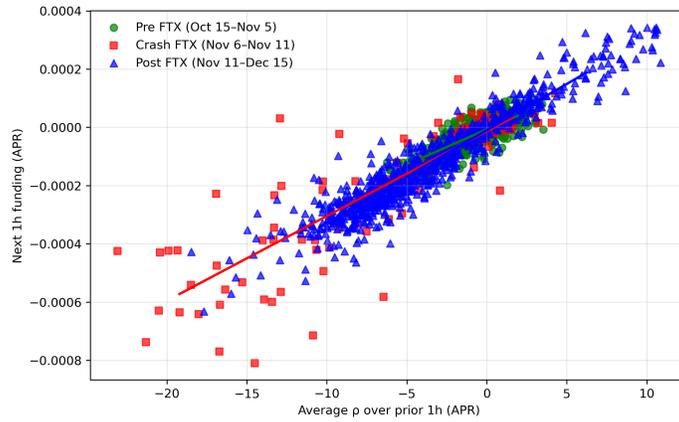
(b) FTX (Nov 6, 2022)
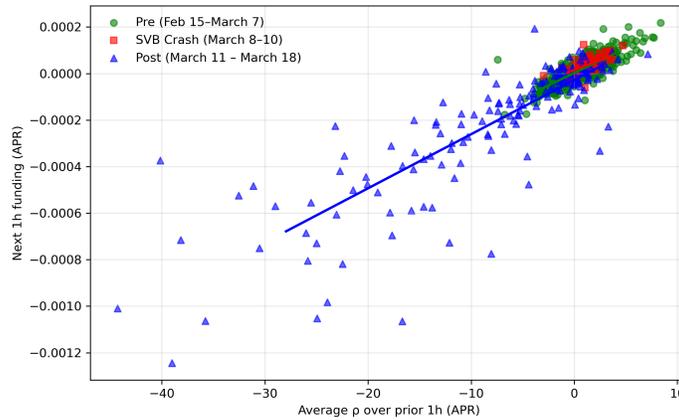
(c) SVB (Mar 10, 2023)

Figure 4: Funding–Basis Elasticity Across Three Stress Episodes

This figure reports the scaled funding–basis elasticity, $\beta_{\mathrm{scaled}} = \beta/\mathrm{median}(f_t/\rho_t)$, for Kraken ETH/USD perpetual swaps during three systemic events: Terra (May 2022), FTX (Nov 2022), and SVB (Mar 2023). The dashed horizontal line marks the benchmark $\beta = 1$. Elasticity collapses during the Terra run but remains above 1 during FTX and SVB, indicating preserved arbitrage function.
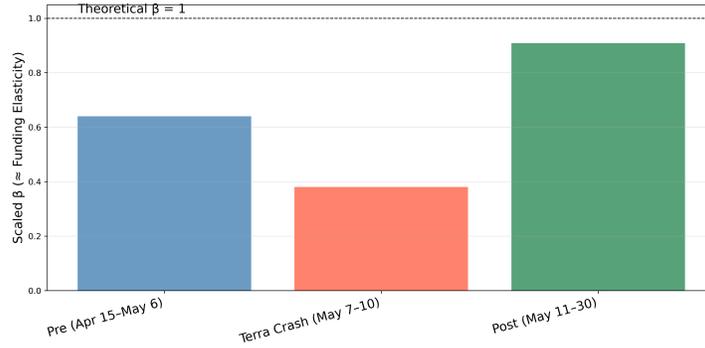
Panel A. Terra Collapse (May 7–10, 2022)
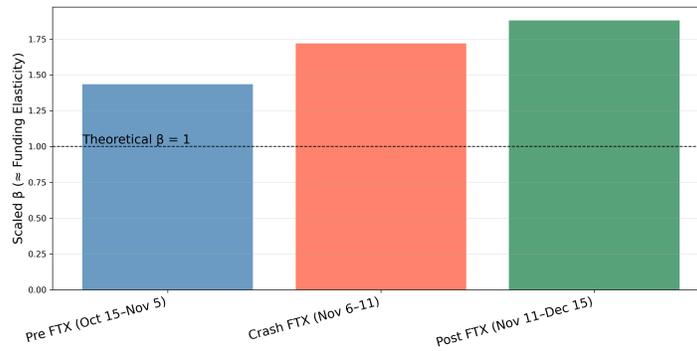
Panel B. FTX Collapse (Nov 6–11, 2022)
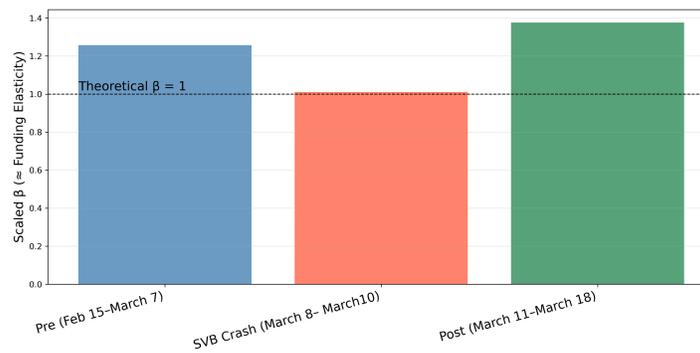
Panel C. SVB Failure (Mar 8–10, 2023)

Figure 5: Ethereum Perps Open Interest Around Major Market Crashes.
Open Interest (notional) for three crisis episodes: (a) Terra collapse (May 2022), (b) FTX collapse (Nov 2022), and (c) SVB collapse (Mar 2023). Shaded regions denote the event windows. The Terra episode shows the steepest decline in Open Interest. The FTX episode shows an increase, while the SVB crash episode shows a slight decline.

(a) Terra Crash Onset (May 7, 2022)

(b) FTX Collapse Onset (Nov 6, 2022)

(c) SVB Collapse Onset (Mar 8, 2023)

33

Figure 6: Ethereum Adverse Selection Costs Around Major Market Crashes.
Adverse Selection Costs (USD) are shown for three crisis episodes: (a) Terra collapse (May 2022), (b) FTX collapse (Nov 2022), and (c) SVB collapse (Mar 2023). Shaded regions denote the event windows. The Terra episode shows a sharp increase in Adverse Selection Costs, followed by the FTX and SVB crash episodes.
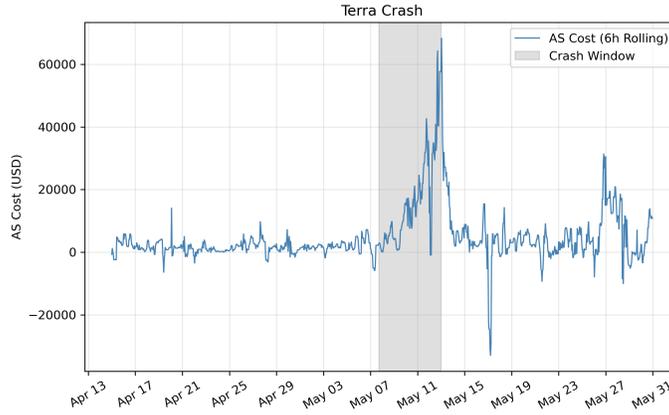
(a) Terra Crash Onset (May 7, 2022)
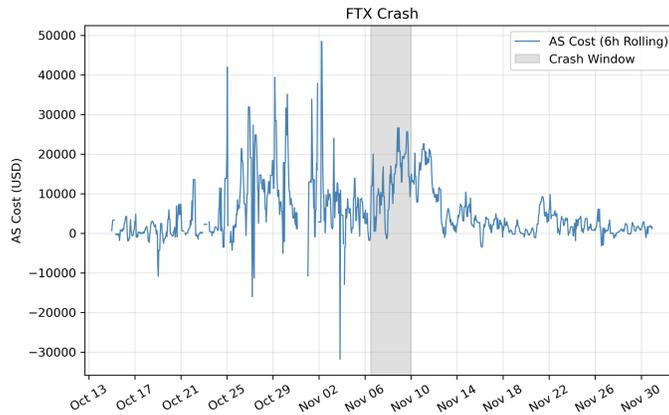
(b) FTX Collapse Onset (Nov 6, 2022)
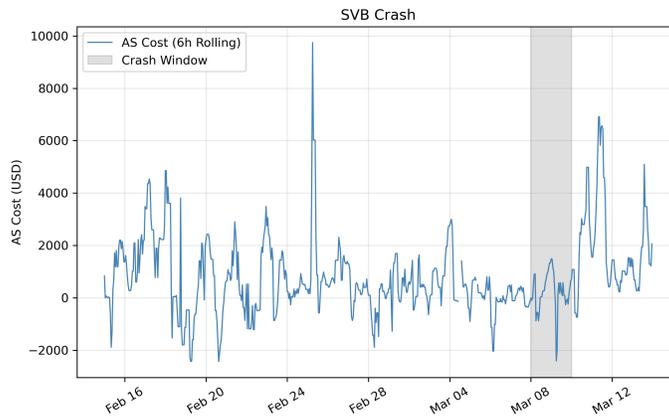
(c) SVB Collapse Onset (Mar 8, 2023)

Figure 7: Volatility – Terra Period

This figure plots hourly Ethereum (ETH) volatility (σ) in percent from April 15 to May 30, 2022, covering the Terra collapse. The series is partitioned into three event windows: Pre-Crash (blue, April 15 - May 7), Crash (red, May 7 - May 12), and Post-Crash (green, May 14 - May 30). The dashed horizontal line at 1.8% marks the volatility threshold σ^* estimated from the global-games model (Table 7). During the Crash window, volatility spikes breached this threshold, triggering a run on open interest.
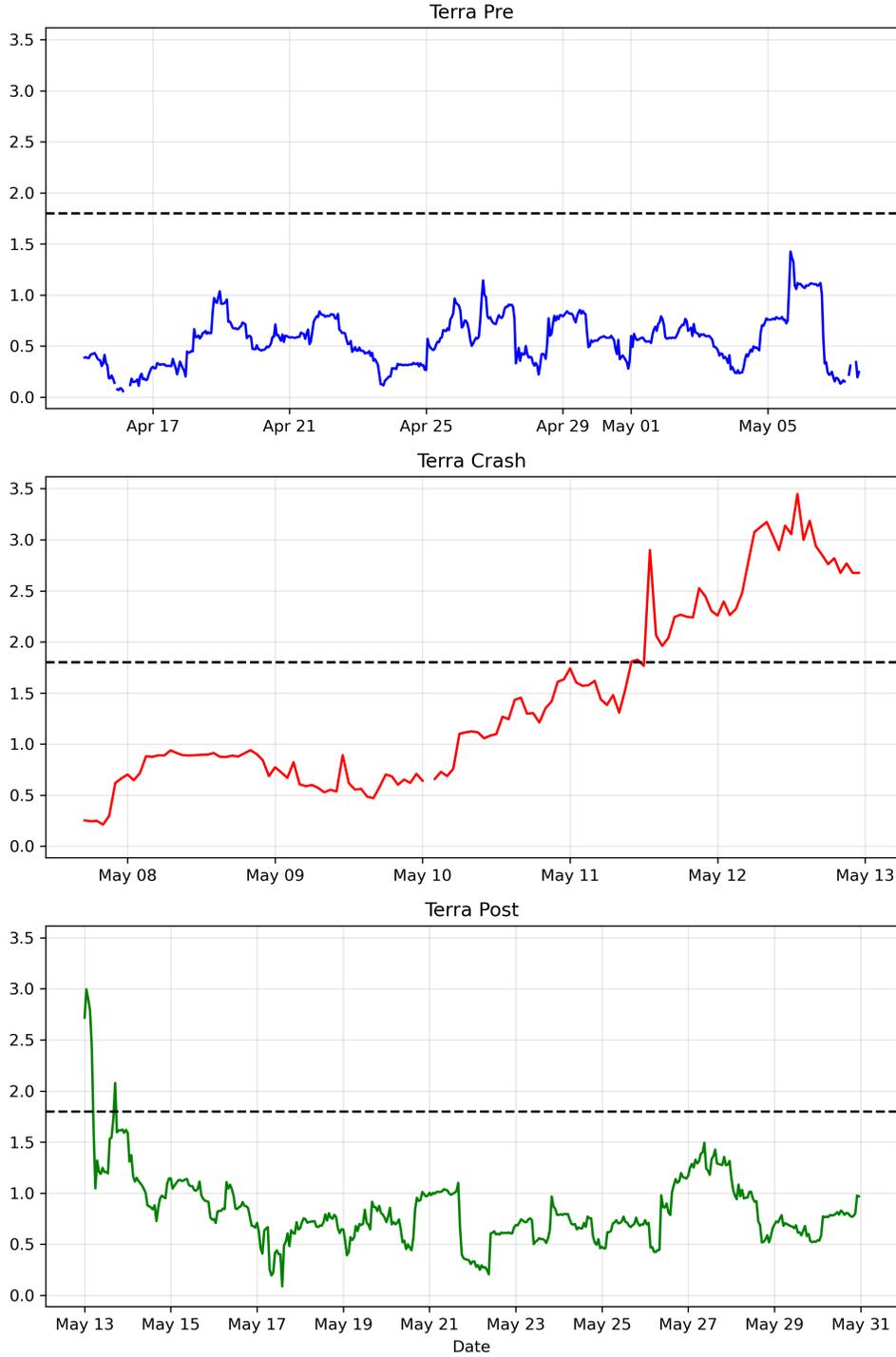
Figure 8: Volatility – FTX Period

This figure plots hourly Ethereum (ETH) volatility (σ) in percent from Oct 15 to Nov 30, 2022, covering the FTX collapse. The series is partitioned into three event windows: Pre-Crash (blue, Oct 15 - Nov 5), Crash (red, Nov 6 - Nov 9), and Post-Crash (green, Nov 10 - Nov 30). The dashed horizontal line at 0.9% marks the volatility threshold σ^* estimated from the global-games model (Table 7). During the Crash window, volatility spikes breached this threshold, but the run was not triggered as σ^* was statistically insignificant.

36
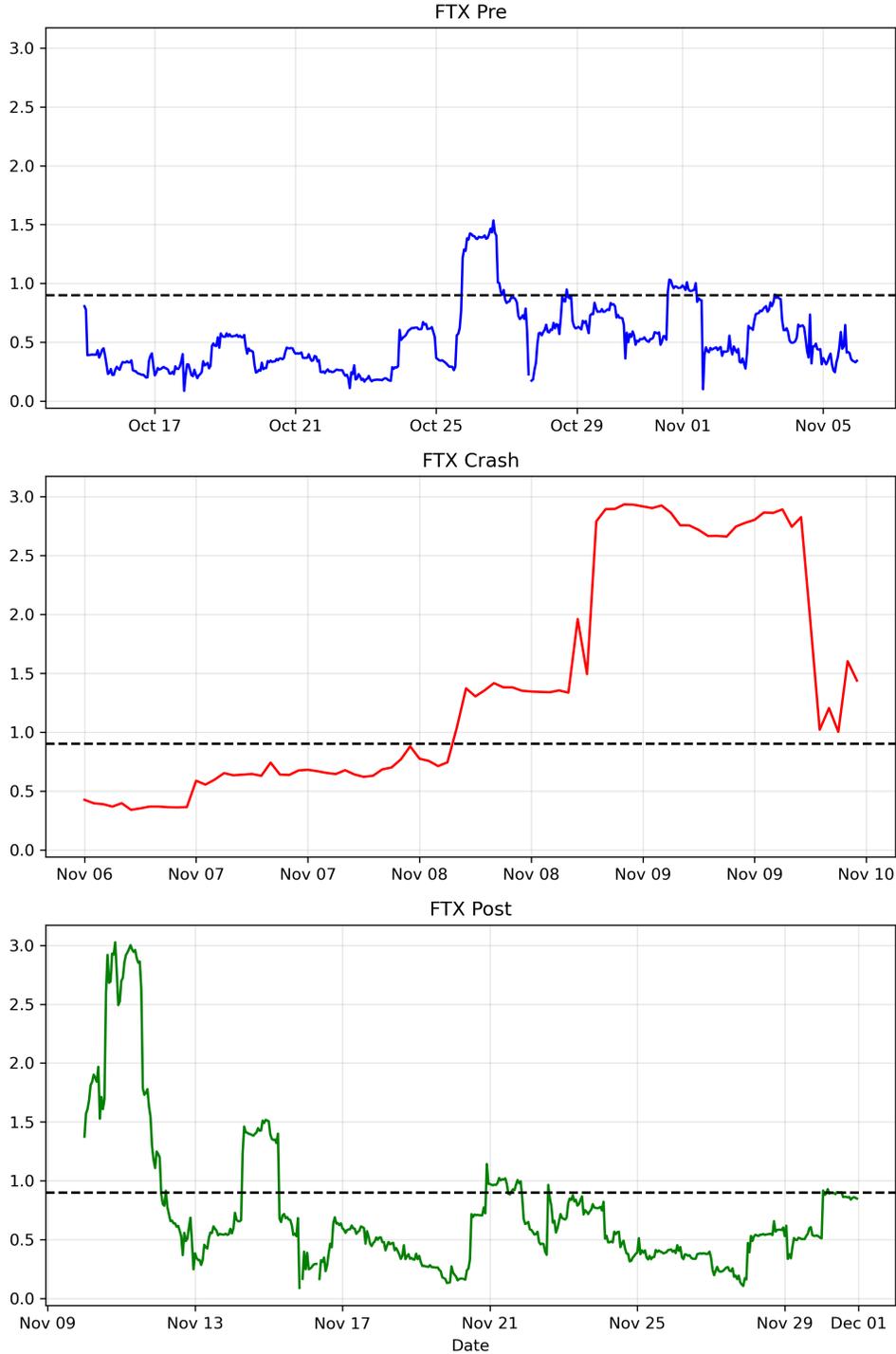
Figure 9: Volatility – SVB Period

This figure plots hourly Ethereum (ETH) volatility (σ) in percent from Feb 15 to March 13, 2023, covering the SVB collapse. The series is partitioned into three event windows: Pre-Crash (blue, Feb 15 - Feb 5), Crash (red, Feb 8 - Feb 9), and Post-Crash (green, Feb 10 - Feb 13). The dashed horizontal line at 1.1% marks the statistically significant volatility threshold σ^* estimated from the global-games model (Table 7), Post Crash. Pre and during the crash window, volatility was below the threshold, and the run was not triggered. Moreover, σ^* was statistically insignificant during these periods (0.6% and -0.1 %).
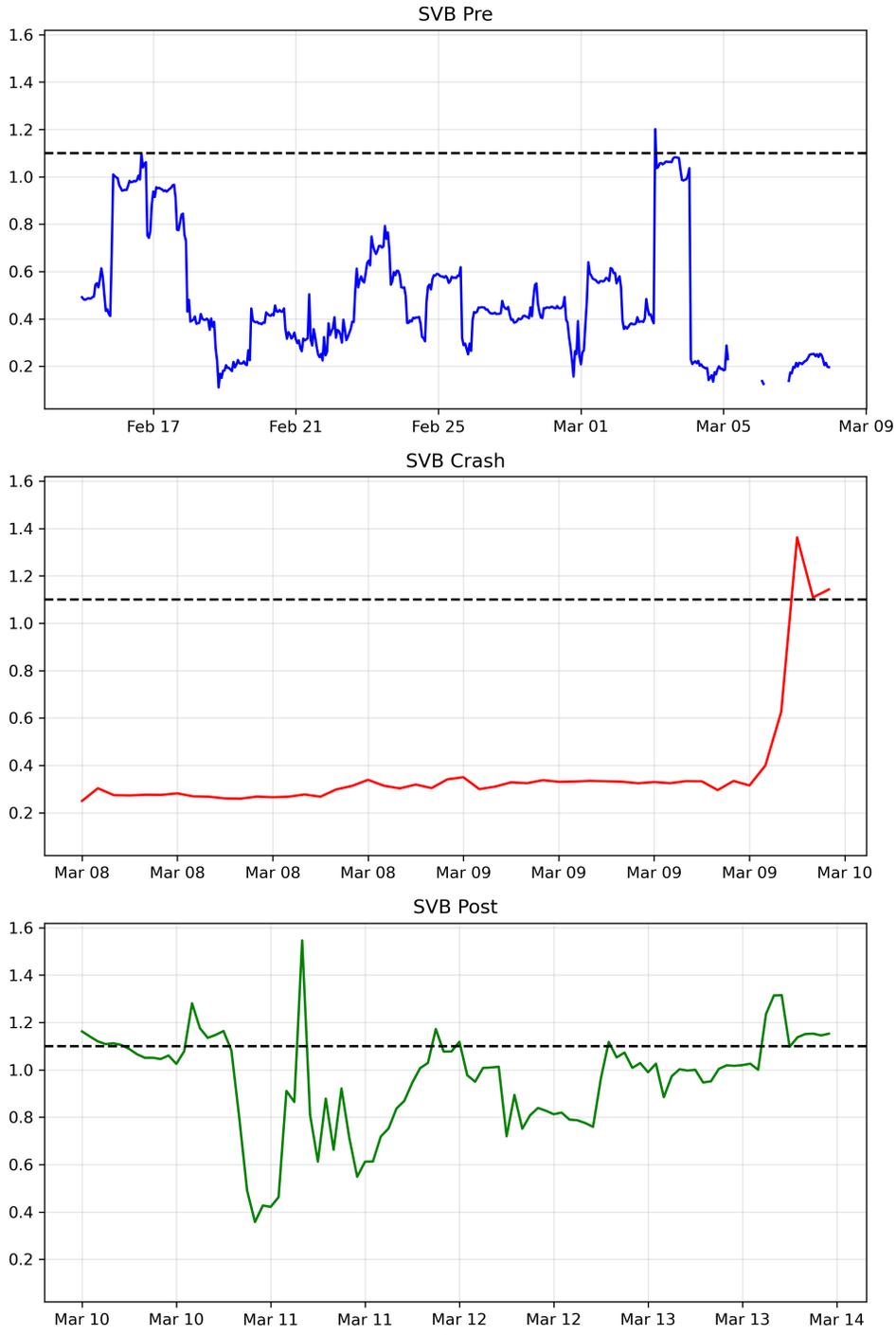
Figure 10: Scaled Funding–Basis Elasticity (β) Across China Crackdown Phases. Each bar shows the scaled funding elasticity ($\beta_{\text{scaled}} = \beta/\text{median}(f_t/\rho_t)$) during the 2021 China cryptocurrency crackdown. The scaled elasticity $\beta_{\text{scaled}} = \beta/\text{median}(f_t/\rho_t)$ with $\text{median}(f_t/\rho_t) = 1.69 \times 10^{-5}$ yields values of 1.5, 0.09, 0.89, 0.53, 0.82, and 0.77 for the respective windows. The elasticity falls sharply to 0.09 during the high–asymmetry Phase I (May 21 –June 10), indicating impaired arbitrage and weak funding–basis linkage, and gradually recovers toward unity once the regulatory stance becomes clearer.
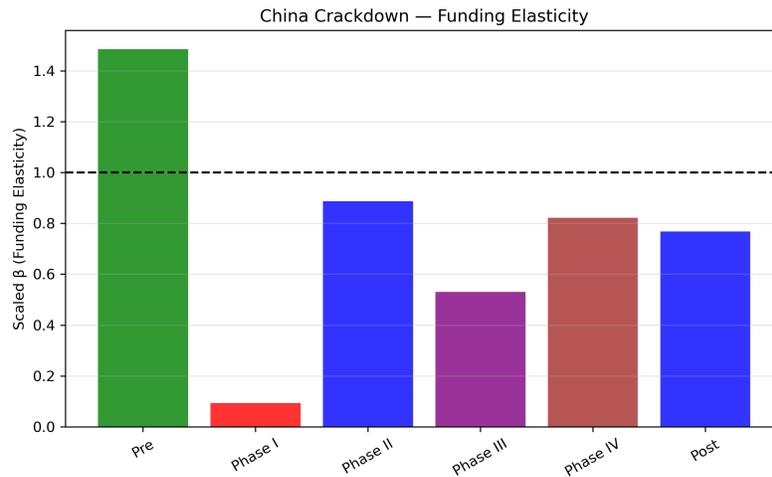
Figure 11: Open Interest Across China Crackdown Phases.
The figure shows the evolution of open interest during the 2021 China cryptocurrency crackdown. Open Interest falls sharply by 80% during the high–asymmetry Phase I (May 21 –June 10), indicating a run on perpetuals, and gradually recovers with a significant capital inflow during Phase IV, as adverse selection costs decline.
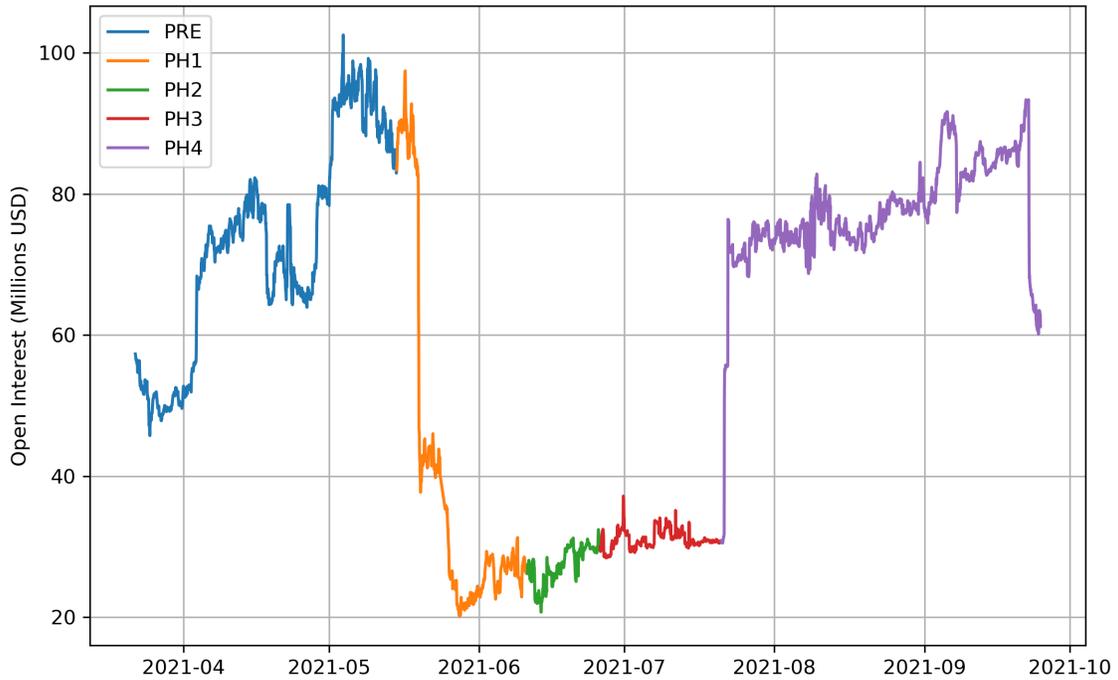
Figure 12: Volatility – China Crypto Ban Period

This figure plots hourly Ethereum (ETH) volatility (σ) in percentage terms from May 15 to September 24, 2021, covering the China Crypto regulatory period. The series is partitioned into four event windows. The dashed horizontal line at 4.64% during Phase I marks the statistically significant volatility threshold σ^* estimated from the global-games model (Table 13). During other phases, σ^* was statistically insignificant, and the run was not triggered despite volatility crossing the threshold.
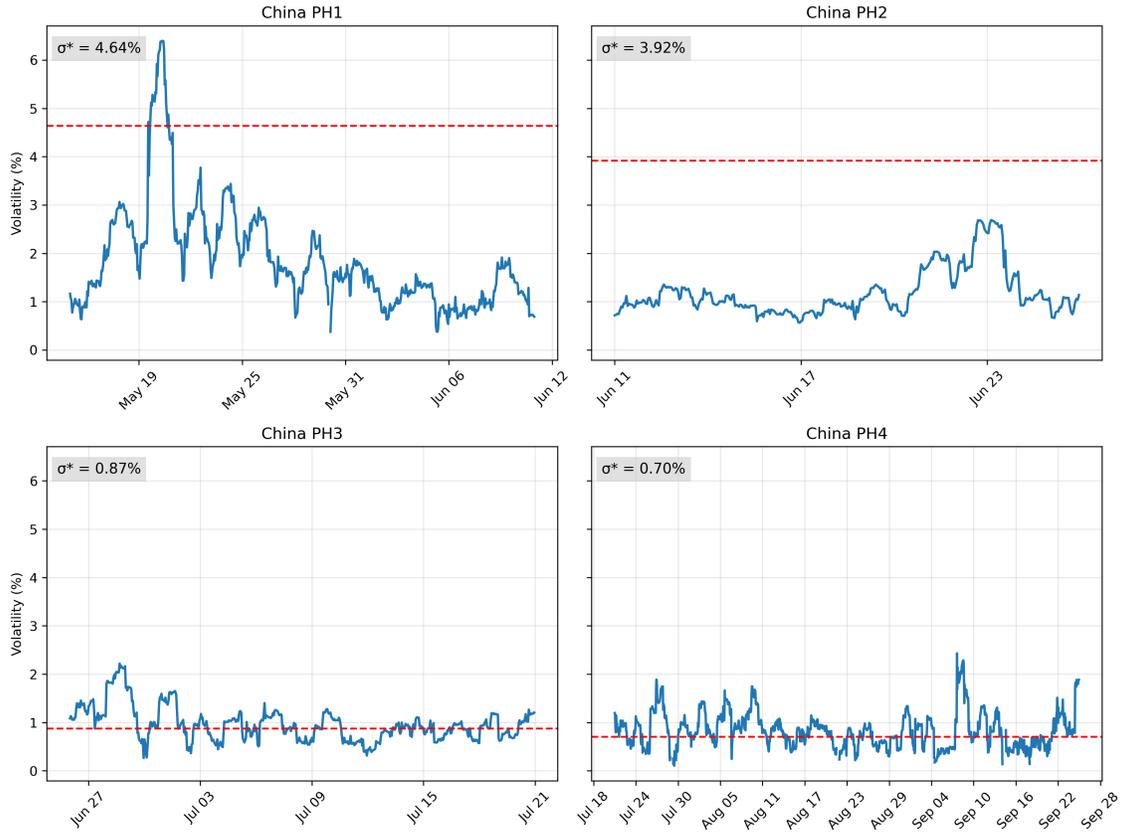
Table 1: Summary Statistics — Ethereum Futures

Panel A: Terra

Variable	Pre Mean	Pre SD	Crash Mean	Crash SD	Post Mean	Post SD
Price	2913.47	120.30	2256.09	216.47	1951.43	100.50
Basis	0.17	0.43	0.32	0.54	-0.05	0.25
Funding Rate	0.002	0.005	0.01	0.01	-0.002	0.01
Spread	1.72	0.37	1.69	0.61	1.18	0.21
AS_cost_10k	0.27	1.84	1.84	2.45	0.36	2.05
Open Interest	58.74	1.14	49.27	18.68	20.30	1.12
σ_{ETH}	0.01	0.002	0.02	0.01	0.01	0.002
Order Flow	-0.002	0.77	-0.07	0.61	0.08	0.74
Momentum	-0.0003	0.01	-0.002	0.02	-0.0001	0.01

Panel B: FTX

Variable	Pre Mean	Pre SD	Crash Mean	Crash SD	Post Mean	Post SD
Price	1442.30	136.87	1376.60	167.36	1234.27	50.08
Basis	-0.11	0.28	-0.85	0.89	-0.47	0.71
Funding Rate	-0.003	0.01	-0.02	0.02	-0.01	0.02
Spread	0.63	0.25	1.30	0.60	0.73	0.22
AS_cost_10k	0.68	2.35	1.40	1.50	0.18	0.58
Open Interest	10.96	0.29	11.33	1.11	11.83	1.19
σ_{ETH}	0.01	0.003	0.02	0.01	0.005	0.003
Order Flow	0.06	0.76	-0.04	0.62	-0.01	0.70
Momentum	0.0004	0.01	-0.002	0.02	0.0000	0.01

Panel C: SVB

Variable	Pre Mean	Pre SD	Crash Mean	Crash SD	Post Mean	Post SD
Price	1630.40	48.99	1484.58	61.26	1534.51	83.52
Basis	0.16	0.42	-0.06	0.69	-2.65	1.94
Funding Rate	0.002	0.01	-0.0003	0.01	-0.05	0.04
Spread	0.43	0.13	0.54	0.19	0.81	0.20
AS_cost_10k	0.07	0.27	0.18	0.32	0.22	0.39
Open Interest	9.36	0.28	9.05	0.29	8.94	0.44
σ_{ETH}	0.005	0.003	0.01	0.004	0.01	0.002
Order Flow	0.10	0.74	-0.25	0.63	0.04	0.55
Momentum	0.0000	0.01	0.001	0.01	0.001	0.01

Table 2: Funding–Basis Elasticity in Normal Times (Nov 2021 – Apr 2022). This table reports monthly regressions of the hourly funding rate (y_t) on the prior-hour basis premium (x_t): $y_t = \alpha + \beta x_t + \varepsilon_t$. Funding and basis are annualized (APR). Coefficients α and β are reported in units of 10^{-5}. Scaled elasticity β_{scaled} normalizes β relative to full pass-through.

	Nov 2021	**Dec 2021**	**Jan 2022**	**Feb 2022**	**Mar 2022**	**Apr 2022**
α ($\times 10^{-5}$)	1.30***	1.04***	−0.501**	1.29***	−0.445**	1.56***
	(6.55)	(7.31)	(−2.21)	(6.03)	(−2.19)	(9.60)
β ($\times 10^{-5}$)	1.34***	0.753***	1.32***	0.990***	1.14***	0.856***
	(17.29)	(9.35)	(10.68)	(7.93)	(9.48)	(7.87)
β_{scaled}	0.79	0.45	0.78	0.59	0.68	0.51
R^2	0.301	0.108	0.137	0.088	0.111	0.082
N	697	721	721	649	721	697

Note: $\beta_{\text{scaled}} = \beta / \text{median}(f_t / \rho_t)$ within each window. Stars denote significance at 10% (*), 5% (**), and 1% (***). T-statistics are reported in parentheses.

Table 3: Funding–Basis Elasticity Across Crisis Episodes. This table reports hourly regressions of next-hour funding (y_t) on the prior-hour basis premium (x_t): $y_t = \alpha + \beta x_t + \varepsilon_t$. Funding and basis are annualized (APR). Coefficients α and β are expressed in units of 10^{-5}. Scaled elasticity $\beta_{\text{scaled}} \equiv \beta/\text{median}(f_t/\rho_t)$ normalizes β so that $\beta_{\text{scaled}} \approx 1$ corresponds to full pass-through.

	Terra Collapse			FTX Collapse			SVB Episode		
	Pre	Crash	Post	Pre	Crash	Post	Pre	Crash	Post
α ($\times 10^{-5}$)	1.44***	8.41***	−0.64**	−0.695***	−1.39	−0.997***	0.235	1.56***	−2.82**
	(7.98)	(9.31)	(−2.26)	(−4.28)	(−1.05)	(−4.44)	(1.54)	(2.76)	(−2.01)
β ($\times 10^{-5}$)	1.08***	0.643	1.53***	2.43***	2.91***	3.18***	2.13***	1.71***	2.33***
	(8.18)	(1.62)	(8.23)	(29.93)	(18.79)	(88.87)	(33.34)	(5.66)	(20.90)
β_{scaled}	0.64	0.38	0.91	1.44	1.72	1.88	1.26	1.01	1.38
R^2	0.113	0.036	0.130	0.641	0.748	0.907	0.689	0.406	0.725
N	528	73	456	504	121	816	504	49	168

Notes: T-statistics in parentheses. Significance levels: $^*p < 0.10$, $^{**}p < 0.05$, $^{***}p < 0.01$. β_{scaled} uses a common empirical scale factor $\text{median}(f_t/\rho_t) = 1.69 \times 10^{-5}$ for comparability across windows.
Event windows: Pre Terra (Apr 15–May 6), Terra Crash (May 7–10), Post Terra (May 11–30); Pre FTX (Oct 15–Nov 5), Crash FTX (Nov 6–11), Post FTX (Nov 11–Dec 15); Pre SVB (Feb 15–Mar 7), SVB Crash (Mar 8–10), Post SVB (Mar 11–18).

Table 4: Adverse Selection Summary Statistics by Event

Statistic	Terra	FTX	SVB
PRE Median	0.185	0.171	0.111
PRE SD	3.495	1.242	0.558
PRE P25	-0.000	-0.029	-0.116
PRE P75	0.392	0.416	0.395
N	455	941	363
CRASH Median	0.313	0.329	0.161
CRASH SD	0.339	0.564	0.503
CRASH P25	0.122	0.168	-0.082
CRASH P75	0.586	0.586	0.357
N	123	73	39
POST Median	0.192	0.140	0.162
POST SD	0.692	0.681	0.315
POST P25	-0.050	-0.046	0.041
POST P75	0.458	0.372	0.331
N	364	824	96

Table 5: Adverse Selection Cost Summary Statistics for Ethereum

Summary statistics are reported for the pre-crisis, crash, and post-crisis windows of the Terra, FTX, and SVB episodes. Adverse selection costs, realized in next hour t, are computed using the median adverse selection estimate between consecutive hours and the corresponding 24-hour trading volume. Specifically, for each hour t, I compute

$$\text{AS Cost}_t = \text{RawAS}_{[t-1 \to t]} \times \left(\frac{\text{Volume}_t^{24h}}{\text{Price}_t} \right),$$

where $\text{RawAS}_{[t-1 \to t]}$ denotes the median adverse-selection component between $t-1$ and t (in USD/ETH), Volume_t^{24h} is the 24-hour notional trading volume (in USD), and Price_t is the spot ETH price (USD/ETH). This yields the total dollar value of informational trading costs in each hourly window.

Statistic	Terra	FTX	SVB
PRE Median	1433.96	1988.55	485.81
PRE SD	18638.99	19967.02	2721.63
PRE P25	-6.20	-277.39	-389.21
PRE P75	3543.42	7196.47	1718.77
PRE N	455	919	363
CRASH Median	12911.05	14561.84	455.97
CRASH SD	24691.19	17277.00	1319.94
CRASH P25	2775.21	5512.76	-228.98
CRASH P75	27179.43	19992.39	990.32
CRASH N	123	73	39
POST Median	3327.19	979.86	1826.78
POST SD	20450.48	5685.78	3894.06
POST P25	-848.34	-290.99	504.67
POST P75	9769.68	3018.78	3344.97
POST N	363	824	96

Table 6: Open Interest Response to Market Forces

	Pre-Crisis	Crisis	Post-Crisis
Panel A: Terra Collapse (May 2022)			
AS_cost$_{t-1}$	−0.040	4.591***	0.174
	(0.141)	(1.286)	(0.132)
Realized Volatility ($\sigma_{ETH,t-1}$)	−133.144***	−370.142**	−11.130
	(24.292)	(152.409)	(26.116)
Momentum (Mom_{t-1})	−5.861	−66.754	−4.186
	(8.886)	(45.946)	(7.056)
Order Flow Imbalance ($OF_{i,t-1}$)	−0.085	0.274	0.171*
	(0.076)	(1.617)	(0.092)
AS_cost$_{t-1} \times \sigma_{ETH,t-1}$	27.073	−257.249***	−27.683*
	(33.698)	(50.142)	(14.760)
Observations	462	122	387
Hourly FE	Yes	Yes	Yes
R^2	0.088	0.640	0.073
Panel B: FTX Collapse (Nov 2022)			
AS_cost$_{t-1}$	−0.026*	0.052	−0.152*
	(0.015)	(0.175)	(0.085)
Realized Volatility ($\sigma_{ETH,t-1}$)	−3.515	71.399***	−24.398**
	(5.184)	(21.686)	(10.569)
Momentum (Mom_{t-1})	0.782	−1.053	6.114
	(2.189)	(8.149)	(4.266)
Order Flow Imbalance ($OF_{i,t-1}$)	0.020	−0.119	0.078
	(0.022)	(0.272)	(0.064)
AS_cost$_{t-1} \times \sigma_{ETH,t-1}$	1.726	−6.062	6.698
	(1.728)	(8.835)	(6.516)
Observations	316	73	446
R^2	0.079	0.431	0.049
Hourly FE	Yes	Yes	Yes

Table continued on next page.

Table 6 (continued)

	Pre-Crisis	Crisis	Post-Crisis
Panel C: SVB Collapse (Mar 2023)			
AS_cost$_{t-1}$	0.171	0.122	1.751***
	(0.146)	(0.393)	(0.541)
Realized Volatility ($\sigma_{ETH,t-1}$)	9.743	−78.825***	25.132
	(6.249)	(16.025)	(28.990)
Momentum (Mom_{t-1})	4.564*	−3.945	11.393***
	(2.561)	(2.230)	(3.801)
Order Flow Imbalance ($OF_{i,t-1}$)	−0.023	−0.034	−0.018
	(0.023)	(0.028)	(0.091)
AS_cost$_{t-1} \times \sigma_{ETH,t-1}$	−27.769	85.659	−157.659***
	(21.123)	(98.908)	(54.488)
Observations	345	39	96
R^2	0.064	0.948	0.285
Hourly FE	Yes	Yes	Yes

Notes: This table reports the impact of market frictions on Ethereum perpetuals open interest during different stress episodes. The dependent variable is hourly open interest (in millions USD). This table reports volatility thresholds estimated from the regression: $OI_t = \alpha + \beta_{AS} \cdot \text{AS\_cost}_{t-1} + \beta_\sigma \cdot \sigma_{t-1} + \beta_{AS \times \sigma} \cdot \text{AS\_cost}_{t-1} \times \sigma_{t-1} + \gamma' X_{t-1} + \text{Hour FE} + \varepsilon_t$. Pre-crisis periods span 30 days before each event, crisis windows are defined as: Terra (May 8-12, 2022), FTX (November 6-9, 2022), SVB (March 8-9, 2023). Pre and Post-crisis periods extend 30 days before and after each event.

Table 7: Spot Volatility Threshold Estimates Across Crash Episodes

This table reports Ethereum spot volatility thresholds estimated from the regression: $OI_t = \alpha + \beta_{AS} \cdot \text{AS\_cost}_{t-1} + \beta_\sigma \cdot \sigma_{t-1} + \beta_{AS \times \sigma} \cdot \text{AS\_cost}_{t-1} \times \sigma_{t-1} + \gamma' X_{t-1} + \text{Hour FE} + \varepsilon_t$. The threshold volatility $\sigma^* = -\beta_{AS}/\beta_{AS \times \sigma}$ represents the level at which the marginal effect of adverse selection costs on open interest is zero. Run is determined based on whether the threshold was breached during any period and whether the coefficient pattern ($\beta_{AS} > 0$, $\beta_{AS \times \sigma} < 0$) indicates a run equilibrium. Only the Terra crash exhibits a statistically significant threshold (1.785% per hour) with the correct sign pattern and threshold breach, consistent with a global-games run equilibrium.

Crisis	Period	β_{AS}	$\beta_{AS \times \sigma}$	Threshold σ^* (%/hour)	Run?
Terra Collapse (May 2022)					
Terra	Pre	−0.040	27.073	0.148	No
		(0.141)	(33.698)		
Terra	**Crash**	**4.591*****	**−257.249*****	**1.785**	**Yes**
		(1.286)	(50.142)		
Terra	Post	0.174	−27.683*	0.628	No
		(0.132)	(14.760)		
FTX Collapse (November 2022)					
FTX	Pre	−0.026*	1.726	1.5	No
		(0.015)	(1.728)		
FTX	Crash	0.052	−6.062	0.9	No
		(0.175)	(8.835)		
FTX	Post	−0.152*	6.698	2.3	No
		(0.085)	(6.516)		
SVB Collapse (March 2023)					
SVB	Pre	0.171	−27.769	0.6	No
		(0.146)	(21.123)		
SVB	Crash	0.122	85.659	-0.1	No
		(0.393)	(98.908)		
SVB	Post	**1.751*****	**−157.659*****	1.1	**Yes**
		(0.541)	(54.488)		

Table 8: Summary of Ethereum Open Interest–Funding Rate Dynamics

This table summarizes the relationship between open interest and funding rates during crash windows across the three crisis episodes. OI Change refers to the change in open interest during the crash window. β Sign and significance refer to the coefficient on lagged open interest in Equation (18).

Crisis	OI Change	β Sign	Significant?	R^2	Interpretation
Terra	−65%	Positive	Yes ($p < 0.01$)	0.098	Run: Investors exit
FTX	+36%	Negative	Yes ($p < 0.01$)	0.318	No run: Investors enter
SVB	−4% (recovered)	Positive	Yes ($p < 0.01$)	0.428	Stress without run

Table 9: Ethereum Open Interest and Funding Rate Dynamics

This table reports OLS regressions of hourly funding rates on lagged open interest (millions USD). Only during the Terra crash phase does the funding rate fail to close the perp–spot basis.

	Terra			FTX			SVB		
	Pre	Crash	Post	Pre	Crash	Post	Pre	Crash	Post
OI_{t-1}	−0.0002	0.0002***	−0.0003	−0.004***	−0.012***	0.003***	0.006***	0.016***	0.026**
	(0.0002)	(0.0001)	(0.0003)	(0.001)	(0.002)	(0.001)	(0.001)	(0.004)	(0.011)
Constant	0.012	−0.003	0.004	0.041***	0.125***	−0.059***	—	—	—
	(0.011)	(0.003)	(0.006)	(0.015)	(0.024)	(0.009)			
Observations	454	122	387	316	73	446	504	72	71
R^2	0.002	0.098	0.003	0.028	0.318	0.028	0.087	0.428	0.198

Table 10: China Ban Phases, Windows, and Adverse Selection (Median AS)

Period	Window / Phase	Info Asymmetry	Median AS
2021-03-22 – 2021-05-20	60-Day Pre	Low	0.339
2021-05-21 – 2021-06-10	Phase I	High	0.712
2021-06-11 – 2021-06-25	Phase II	Medium	0.470
2021-06-26 – 2021-07-20	Phase III	Medium	0.416
2021-07-21 – 2021-09-24	Phase IV	Declining	0.330
2021-09-25 – 2021-11-23	60-Day Post	Low	0.510

Table 11: Funding–Basis Elasticity During China's Cryptocurrency Crackdown. This table reports hourly regressions of the next-hour funding rate (y_t) on the prior-hour basis premium (x_t), $y_t = \alpha + \beta x_t + \varepsilon_t$. Funding and basis are annualized in APR. Coefficients α and β are reported in units of 10^{-5}. The scaled elasticity β_{scaled} normalizes β relative to $\beta = 1$.

	Pre	Phase I	Phase II	Phase III	Phase IV	Post
	(Mar 22–May 20)	(May 21–Jun 10)	(Jun 11–Jun 25)	(Jun 26–Jul 20)	(Jul 21–Sep 24)	(Sep 25–Nov 23)
	(1)	(2)	(3)	(4)	(5)	(6)
α ($\times 10^{-5}$)	14.1***	−0.347	−3.91***	0.815**	4.03***	2.35***
	(16.62)	(−0.46)	(−5.91)	(2.36)	(17.78)	(14.97)
β ($\times 10^{-5}$)	2.51***	0.156	1.50***	0.896***	1.39***	1.30***
	(24.39)	(0.94)	(6.57)	(5.13)	(16.66)	(21.34)
β_{scaled}	1.48	0.09	0.89	0.53	0.82	0.77
R^2	0.296	0.002	0.114	0.044	0.151	0.244
N	1417	458	337	577	1561	1417

Note: β_{scaled} is computed as $\beta/\text{median}(f_t/\rho_t)$ within each window. *Event windows:* Pre (Mar 22–May 20), Phase I (May 21–Jun 10), Phase II (Jun 11–Jun 25), Phase III (Jun 26–Jul 20), Phase IV (Jul 21–Sep 24), Post (Sep 25–Nov 23).

Table 12: Open Interest Response to Adverse Selection Costs and Market Frictions Across China Ban Phases

This table reports the impact of market frictions on Ethereum perpetuals open interest during different stress episodes estimated from the regression: $OI_t = \alpha + \beta_{AS} \cdot \text{AS\_cost}_{t-1} + \beta_\sigma \cdot \sigma_{t-1} + \beta_{AS \times \sigma} \cdot \text{AS\_cost}_{t-1} \times \sigma_{t-1} + \gamma' X_{t-1} + \text{Hour FE} + \varepsilon_t$. The dependent variable is hourly open interest (in millions USD). Adverse selections costs are per 10k USD. Pre and Post-crisis periods extend 30 days before and after each event.

	Pre	PH1	PH2	PH3	PH4	Post
AS_Cost_t-1	0.309**	1.987***	0.098	−0.054	−0.185	−0.211
	(0.150)	(0.237)	(0.094)	(0.038)	(0.115)	(0.198)
Sigma_ETH_t-1	344.968***	609.467***	147.568***	−52.156***	−517.055***	−1,076.180***
	(103.238)	(144.538)	(35.370)	(19.432)	(66.920)	(95.455)
Mom_t-1	36.561	−50.296	−5.206	−1.780	−44.021**	−20.818
	(35.971)	(46.107)	(12.050)	(6.015)	(22.244)	(36.145)
OF_i_t-1	0.900	1.538	−0.441*	0.006	−0.404	0.415
	(0.685)	(1.675)	(0.227)	(0.095)	(0.363)	(0.471)
AS_Cost_t-1 × Sigma_t-1	13.979	−42.837***	−2.502	6.198*	26.362**	39.400*
	(10.669)	(9.181)	(6.097)	(3.709)	(11.159)	(20.600)
Observations	1,194	616	348	480	1,457	1,353
R^2	0.079	0.164	0.129	0.038	0.050	0.092
Hour FE	Y	Y	Y	Y	Y	Y

Table 13: Spot Volatility Threshold Estimates — China Cryptocurrency Ban (2021)

This table reports Ethereum spot volatility thresholds estimated from the regression: $OI_t = \alpha + \beta_{AS} \cdot \text{AS\_cost}_{t-1} + \beta_{\sigma} \cdot \sigma_{t-1} + \beta_{AS \times \sigma} \cdot \text{AS\_cost}_{t-1} \times \sigma_{t-1} + \gamma' X_{t-1} + \text{Hour FE} + \varepsilon_t$. The threshold volatility $\sigma^* = -\beta_{AS}/\beta_{AS \times \sigma}$ represents the level at which the marginal effect of adverse selection costs on open interest is zero. Threshold volatility is defined as $\sigma^* = -\beta_{AS}/\beta_{AS \times \sigma}$. A "Run" is recorded only when: (i) $\beta_{AS} > 0$ and $\beta_{AS \times \sigma} < 0$ with $p < 0.01$, and (ii) the realized volatility in the event window crosses σ^*. Only Phase I satisfies both conditions, indicating a withdrawal of open interest during the China crypto ban regulatory period.

China Phase	β_{AS}	$\beta_{AS \times \sigma}$	Threshold σ^* (%/hour)	Run?
PRE	0.309**	13.979	–	No
	(0.150)	(10.669)		
I	**1.987*****	**−42.837*****	**4.6**	**Yes**
	(0.237)	(9.181)		
II	0.098	−2.502	3.9	No
	(0.094)	(6.097)		
III	−0.054	6.198*	0.9	No
	(0.038)	(3.709)		
IV	−0.185	26.362**	0.7	No
	(0.115)	(11.159)		
POST	−0.211	39.400*	0.5	No
	(0.198)	(20.600)		

Appendix

A Perpetual Pricing Terminology – Kaiko Data

Index Price

The *index price* represents the reference spot value of ETH/USD. It is computed by Kraken as a time-weighted median of ETH/USD spot prices across major exchanges (e.g., Coinbase, Bitstamp, and Kraken Spot). The index price serves as the contract's anchor and is intended to reflect the fair market value of the underlying asset. Because it aggregates multiple venues, the index price is robust to idiosyncratic noise or manipulation on any single exchange.

Mark Price

The *mark price* is the exchange's internal fair-value estimate of the perpetual contract. It is not the last trade price but a smoothed measure used for mark-to-market profit and loss calculations and for determining funding payments and liquidation triggers. Kraken defines:

$$\text{Mark Price}_t = \text{Index Price}_t \times (1 + \text{Premium Index}_t), \tag{19}$$

where the *Premium Index* is a rolling weighted average of the percentage difference between the perpetual's traded price and the index price over the recent interval. As a result, the mark price tracks the index price closely but adjusts for persistent deviations between the two markets.

Funding Rate

The *funding rate* is the periodic interest-like payment exchanged between long and short positions that keeps the perpetual price anchored to its spot reference. When the perpetual trades above the index price (*positive basis*), the funding rate is positive, causing longs to pay shorts. Conversely, when the perpetual trades below the index (*negative basis*), the funding rate is negative, and shorts pay longs. The funding mechanism therefore enforces convergence between the perpetual and spot

markets:

$$\text{Funding Rate}_t = \text{Interest Adjustment}_t + \text{Premium Index}_t, \tag{20}$$

$$f_t > 0 \implies \text{longs pay shorts}, \quad f_t < 0 \implies \text{skurthorts pay longs}. \tag{21}$$

Relation to the Spot Market

The difference between the mark and index prices,

$$\rho_t = \ln(\text{Mark Price}_t) - \ln(\text{Index Price}_t),$$

is the *perpetual basis*—a measure of the deviation of the futures market from its spot reference. Arbitrageurs monitor this basis and exploit positive or negative spreads through offsetting positions in the spot and perpetual markets. The funding mechanism, by periodically adjusting cash flows between longs and shorts, serves as an endogenous force driving ρ_t toward zero. In equilibrium, the mark price should closely track the index price, and funding payments adjust to enforce this parity. Temporary deviations—such as those observed during the May 2022 Terra collapse—reflect transient limits to arbitrage or liquidity constraints in the perpetual market.

B   Institutional Background

B.1   Cryptocurrency Spot Markets

The cryptocurrency spot market, where assets are traded for immediate delivery, has evolved from a retail-dominated niche into a complex institutional-grade ecosystem. This transformation is driven by advancements in market infrastructure, regulatory clarity, and the development of sophisticated financial instruments. The core of the spot market involves the immediate exchange of a cryptocurrency, such as Bitcoin or Ethereum, for fiat currency (e.g., USD) or another digital asset. Unlike derivatives, which derive value from an underlying asset, a spot transaction confers immediate ownership. The price at which this exchange occurs is the spot price. By mid-2025,

over 19,000 tokens were listed, yet market value remains highly concentrated in Bitcoin (BTC) and Ethereum (ETH). According to CoinMarketCap's Q2 2025 update, the total crypto market capitalisation was about US $4 trillion, with 24-hour spot trading volume of roughly US $98 billion[5]. CoinGecko's Q3 2025 industry report notes that the market cap continued its upward trajectory in Q3, increasing by 16.4% to end the quarter at around US $4.0 trillion [6]. Binance remains the largest spot exchange, recording roughly US $2 trillion in spot volume in Q3 2025. Binance remains the largest spot exchange, recording roughly US $2 trillion in spot volume in Q3 2025.

B.2 Development of Cryptocurrency Derivative Markets

The first regulated Bitcoin futures began trading on Cboe on 10 December 2017 and on CME on 18 December 2017 under CFTC oversight. CME later introduced cash-settled Ethereum futures on 8 February 2021 [7]. In October 2021, ProShares launched the first U.S. Bitcoin futures-based ETF (BITO), whose first-day trading volume exceeded $1 billion, signaling strong institutional demand.

By 2025, crypto derivatives account for roughly 75–85% of total crypto trading activity. TokenInsight's [8] report notes that derivatives trading on CEXs surged to US $26.0 trillion in Q3 2025, with average daily volume US $283 billion, while spot trading volume was US $4.7 trillion. Global open interest was around US $91 billion, although Coindesk reported that open interest across CEXs reached US $187 billion in August 2025. Derivatives account for the majority of crypto trading. Kaiko data show that perpetual contracts alone represented 68% of Bitcoin derivative volume. On CME, Bitcoin options open interest reached $4 billion by Q2 2025, and Ether options daily volume increased 65% year-on-year.

B.3 Perpetual-Futures Markets

Perpetual futures (*perps*) are non-expiring contracts that use an eight-hourly *funding rate* mechanism to anchor prices to the spot market. When the perpetual price exceeds spot, longs pay shorts; when below, shorts pay longs. This continuous payment enforces convergence between the two markets.

---

[5] https://coinmarketcap.com/academy/article/according-to-cmc-q2-2025
[6] https://www.coingecko.com/research/publications/2025-q3-crypto-report#:~:text=1,0T%20in%202025%20Q3
[7] https://www.cmegroup.com/media-room/press-releases/2021/2/08/cme_group_announceslaunchofetherfutures.html
[8] https://tokeninsight.com/en/research/reports/crypto-exchanges-report-q3-2025

Perpetuals, first introduced by BitMEX in 2016, now dominate crypto derivatives. CoinGecko's *State of Crypto Perpetuals Report (2025)* [9] estimates that the top ten centralized exchanges traded about $58.5 trillion in perpetual futures during 2024, doubling 2023's figure, with open interest reaching $131 billion in December 2024. Kaiko estimates that derivatives represent over 75 % of total crypto trading activity, with perps alone making up 68 % of Bitcoin trading volume in 2025 [10]. Decentralized perpetual protocols such as dYdX, Hyperliquid, and Aster handled over $1.5 trillion of trading in 2024, with DEX perpetual volumes growing 87% quarter-on-quarter to $1.81 trillion in Q3 2025.

Regulatory Developments. Until 2025, perpetual contracts were offered mainly on offshore platforms. On 21 July 2025, Coinbase Derivatives launched the first U.S.-regulated nano BTC and ETH perpetual futures under the Commodity Futures Trading Commission (CFTC) self-certification. The CFTC did not object, confirming compliance with the Commodity Exchange Act, while the SEC did not challenge ETH's commodity classification [11].

B.3.1 Market Metrics (2025)

Metric	Value	Source
Total crypto market capitalization (Q3 2025)	$4.0 trillion	CoinGecko (2025)
Stablecoin market capitalization	$288 billion	CoinGecko (2025)
Spot trading volume (Q3 2025)	$5.1 trillion	CoinGecko (2025)
Derivatives trading volume (Q3 2025)	$26 trillion	TokenInsight (2025)
Perpetual futures volume (2024)	$58.5 trillion	CoinGecko (2025)
Perpetual open interest (Dec 2024)	$131 billion	CoinGecko (2025)
Perpetual DEX volume (Q3 2025)	$1.81 trillion	CoinGecko (2025)
Global derivatives open interest (Q3 2025)	$91–187 billion	Coindesk (2025)
Crypto options market monthly volume	$8.94 trillion	CoinLaw (2025)

Table 14: Key market metrics for crypto spot, derivatives, and perpetual futures markets as of 2025.

The institutional landscape of crypto markets in 2025 is characterised by enormous spot and derivatives activity, evolving regulatory frameworks, and rapid innovation. Perpetual futures have

[9] https://assets.coingecko.com/reports/2025/CoinGecko-State-of-Crypto-Perpetuals-Market.pdf
[10] https://www.kaiko.com/reports/perps-are-coming-to-america
[11] https://www.pillsburylaw.com/en/news-and-insights/cftc-perpetual-futures-btc-eth-crypto-derivatives.html

become the most popular derivative instrument due to their flexibility and leverage. Global regulators are gradually integrating crypto assets into existing market structures: the EU's MiCA and U.S. legislation, such as the GENIUS and CLARITY Acts, aim to clarify which tokens are commodities or securities and to provide regulatory oversight. The approval of spot Bitcoin and Ether ETFs in 2024 and the launch of the first U.S.-regulated perpetual futures in 2025 mark significant milestones.